INSTITUTE FOR FUSION STUDIES

DE-FG05-80ET-53088-710 IFSR #710

Elliptical Vortices in Shear: Hamiltonian Moment Formulation and Melnikov Analysis

KEITH NGAN
Dept. of Physics, Univ. of Toronto
Toronto, ON, M5S 1A7, Canada

STEVE MEACHAM
Dept. of Oceanography, Florida State Univ.
Tallahassee, FL 32306-3048

and P.J. MORRISON
Institute for Fusion Studies
The University of Texas at Austin
Austin, Texas 78712 USA

July 1995

THE UNIVERSITY OF TEXAS

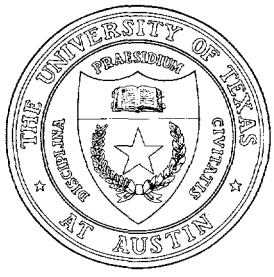

AUSTIN

Elliptical vortices in shear: Hamiltonian moment formulation and Melnikov analysis

Keith Ngan,[a] Steve Meacham,[b] and P. J. Morrison[c]

Abstract

The equations of motion for interacting, elliptical vortices in a background shear flow are derived using a Hamiltonian moment formulation. The equations reduce to the 6th order system of Melander *et al.* [J. Fluid Mech. **167**, 95 (1986)] when a pair of vortices is considered and shear is neglected. The equations for a pair of identical vortices are analyzed with a number of methods, with particular emphasis on the basic interactions and on the implications for vortex merger. The splitting distance between the stable and unstable manifolds connecting the hyperbolic fixed points of the intercentroidal motion—the separatrix splitting—is estimated with a Melnikov analysis. This analysis differs from the standard time-periodic Melnikov analysis on two counts: (a) the "periodic" perturbation arises from a second degree of freedom in the system which is not wholly independent of the first degree of freedom, the intercentroidal motion; (b) this perturbation has a faster time scale than the intercentroidal motion. The resulting Melnikov integral appears to be exponentially small in the perturbation as the latter goes to zero. Numerical simulations, notably Poincaré sections, provide a global view of the dynamics and indicate that there are two modes of merger. The effect of the shear on chaotic motion and on chaotic scattering is also discussed.

[a] Department of Physics, University of Toronto, Toronto, ON, M5S 1A7, Canada
[b] Dept. of Oceanography, Florida State University, Tallahassee, FL 32306-3048.
[c] Department of Physics and Institute for Fusion Studies, University of Texas, Austin, TX 78712

I. INTRODUCTION

In this paper, we present a simple approximate model of the dynamics of N elliptical vortices in a two-dimensional shear flow. Our model has many similarities with other reduced vortex models, most notably with the uniform elliptical vortex in shear of Kida (1981)[1] and the interacting elliptical vortices of Melander *et al.* (1986)[2] (hereafter MZS). What distinguishes our model is the simultaneous presence of vortex-vortex and vortex-shear interactions. These processes complement and compete with one another, resulting in some extremely complex behavior. In deriving our model, we follow the procedure of Flierl *et al.* (1995)[3] (hereafter FMM); we begin with a Hamiltonian description of the full (infinite-dimensional) system and make approximations within this Hamiltonian framework so as to obtain a reduced Hamiltonian description. In this way, the Hamiltonian structure of the problem is preserved in a natural way.

Vortex-vortex and vortex-shear interactions may be found in many different contexts, but they are especially common in geophysics. Nearly homogeneous potential vorticity eddies are common in the atmosphere[4] and ocean,[5–6] and they are an important component of large-scale atmosphere-ocean dynamics. The occlusion of large amplitude meanders on strong atmospheric or oceanic jets often leads to the formation of relatively long-lived eddies. The emergence of quasi-uniform vortices and their complex interaction with one another has been recognized as an important feature of freely-decaying geostrophic (two-dimensional) turbulence.[7–9]

In our model, vortex merger is the combined result of vortex-vortex and vortex-shear interactions. In the absence of any external flow, like-signed vortices will orbit around one other when far apart, but merge when sufficiently close together.[10–12] When there is background shear, it is possible for well-separated vortices to merge if they are oriented

appropriately. Furthermore, these two basic interactions can also interfere with one another: the shear flow may sweep the vortices past one another before they can merge; or each vortex may advect the other around itself, enabling the shear to separate them.

Vortex merger provides much of the physical motivation for this study, but we are not concerned with vortex merger *per se*. We derive the equations of motion for our new model and we attempt to elucidate some aspects of its rather complex behavior. Because of its physical relevance, we have chosen vortex merger to be a unifying theme in our analysis; but it is not the primary focus of this study. The analysis addresses: the relative importance of the different physical processes; whether it is possible to make any predictions about chaotic motion; and some interesting dynamical phenomena which are unrelated to vortex merger (e.g. chaotic scattering).

Our model is obtained by generalizing that of MZS to include a background shear flow; it is essentially a model of N interacting Kida-like vortices. Like MZS, we approximate the vortices as elliptical patches of uniform vorticity and employ an expansion based on spatial moments of the vorticity distribution. However, our derivation of the resulting Hamiltonian system is considerably different. Instead of deriving the equations of motion by manipulating the moments, we follow FMM and utilize methods from noncanonical Hamiltonian dynamics.[13–14]

As with MZS, this model is an approximate one. We assume that the vortices are small and well-separated and that they remain elliptical for all time. The model is consistent as long as the distance between vortex centers is larger than the vortex dimensions. It loses its asymptotic consistency when the vortices are very close; deviations from ellipticity are higher order corrections to the equations of motion. The model cannot accurately describe the details of vortex merger because it assumes that the vortices always remain elliptical; during a vortex merger event, the vortices deviate increasingly from ellipticity. Dritschel and Legras (1991)[12] have shown that a higher order, non-Hamiltonian model (their "elliptical

model with disturbances") gives a better approximation to some of the deformations seen during merger. A Hamiltonian moment method cannot capture these processes completely, but in the absence of external strain, both the elliptical model and the model of MZS give similar predictions for the onset of merger. Thus, despite its limitations, there is reason to hope that the model considered in this paper should provide some insight into the interaction of uniform vortices in shear.

Noncanonical methods have proven to be useful in several branches of continuum mechanics, notably geophysical fluid dynamics[15–16] and magnetohydrodynamics.[17–18] The noncanonical formalism readily lends itself to a systematic procedure for approximating the equations of motion. A simple noncanonical representation of the Hamiltonian structure of the general inviscid and nondiffusive fluid equations involves writing the equations of motion in the form

$$\frac{\partial Z}{\partial t} = \{Z, H\}, \tag{1}$$

where $Z(\mathbf{x}, t)$ is the appropriate set of fluid variables (e.g. $\rho\mathbf{u}$, $\rho, \ldots$), and $H[Z]$ is a Hamiltonian functional. In an Eulerian description, the noncanonical Poisson bracket, $\{\ ,\ \}$, has the form

$$\{F, G\}[Z] = \left\langle Z, \left[\frac{\delta F}{\delta Z}, \frac{\delta G}{\delta Z}\right]\right\rangle, \tag{2}$$

where F and G are functionals, $\langle\ ,\ \rangle$ is an integration over the volume corresponding to the spatial variable $\mathbf{x}$, and the functional derivative is defined by

$$\delta F[Z; \delta Z] =: \left\langle \delta Z, \frac{\delta F}{\delta Z}\right\rangle. \tag{3}$$

The bracket of (2) is a Lie algebra product for functionals, i.e. is bilinear, antisymmetric, and satisfies the Jacobi identity, $\{F, \{G, H\}\} + \{G, \{H, F\}\} + \{H, \{F, G\}\} = 0$, provided the "inner bracket" $[\ ,\ ]$ is a Lie algebra product for functions. In the present context, the $[\ ,\ ]$ corresponds to the horizontal Jacobian. Brackets of the form of (2) are called Lie-Poisson brackets.

The Poisson bracket can be simplified in situations where we can confine our attention to a special subset of all admissible functionals F and G. Specifically, for *functions*, f and g, of a finite set of linear functionals of Z, the Poisson bracket may be written as

$$\{f,g\}(z) = z^{\ell} c_{\ell}^{jk} \frac{\partial f}{\partial z^j} \frac{\partial g}{\partial z^k}, \qquad j,k,\ell = 1,2,\ldots M, \tag{4}$$

where the z^j are the new "dynamical variables," and the quantities c_{ℓ}^{jk} are the structure constants of some Lie algebra. Repeated sum notation is used here (and henceforth). The cosymplectic matrix, $J^{jk} := z^{\ell} c_{\ell}^{jk}$, inherits the property of skew-symmetry and it automatically guarantees Jacobi's identity for the reduced bracket. Using (1) and (4) to obtain equations of motion for the dynamical variables,

$$\dot{z}^j = J^{jk} \frac{\partial H}{\partial z^k}. \tag{5}$$

The main difficulty in applying the finite-dimensional noncanonical formalism is in determining the cosymplectic matrix. In this work, we use a Hamiltonian reduction method, similar to that of FMM, to re-express, exactly, the Poisson bracket for two-dimensional Euler flow in terms of a reduced set of dynamical variables: the first and second order vorticity moments. The idea of reduction has a long pedigree dating to Jacobi and Poincaré.[19–20] Here, reduction allows us to transform an infinite-dimensional system into a finite-dimensional one. The Hamiltonian nature of the equations of motion is more explicit, and the derivation somewhat simpler, than in MZS because of reduction and the noncanonical formalism.[21]

In Sec. II, the cosymplectic matrix and the Hamiltonian are computed for a system of N elliptical vortices in shear. We obtain a system of coupled first order ODE's describing the vortices' quadratic moments and their centroidal motion. A system analogous to that of MZS is obtained by transforming from moment variables to physical variables.

In Sec. III, we nondimensionalize the equations and provide a physical interpretation of them. We isolate the physical processes present and assess their relative importance,

restricting ourselves to a system of two vortices in order to facilitate the analysis. The resulting 4th order, nonlinear system is still difficult to analyse, but considerable insight into the model's behavior may be gained by comparing it to some integrable models: (i) a pair of isolated Kida vortices; (ii) the MZS model for $N = 2$; and (iii) a point vortex pair in shear. Some features of the first two models have been mentioned already; the third model is, for sufficiently strong strain, distinguished by the presence of a separatrix dividing closed orbits (the vortices rotate around one another) from unbounded ones (the vortices separate). Differences between the dynamics of our model and the integrable ones are a consequence of the additional physical processes present in the former. Any of these three models could be used as the basic state for an analysis; we have chosen the point vortex pair in shear because its phase space geometry provides a useful conceptual framework. For the cases we are interested in, closed concentric orbits fill the region from the origin (where the vortices coincide) to the separatrix (see Fig. 1 and the Appendix); the fate of these orbits under a perturbation is essential to vortex merger. The motion around the perturbed separatrix is also of interest: for nonintegrable perturbations, the stable and unstable manifolds associated with the hyperbolic fixed points no longer coincide,[22] the separatrix splits apart and the component manifolds intersect transversally, leading to chaotic motion and transport across the (unperturbed) separatrix.[23–25]

We compute an approximation to the separatrix splitting analytically by performing a Melnikov analysis (Sec. IV). The Melnikov function forms part of an estimate of the separation between the stable and unstable manifolds for a weakly perturbed dynamical system; zeros of the Melnikov function are indicative of transverse intersections of the two manifolds and thus chaotic motion. The problem considered here is not quite the same as the standard Melnikov problem for two reasons: the perturbation expands the phase space, and the perturbation has a time scale much shorter than that of the unperturbed motion. The second of these suggests that the Melnikov integral will be exponentially small,[26] and

this is what we find.

In Sec. V, numerical simulations are presented. Poincaré sections are computed in order to provide a global picture of the dynamics. Vortex merger for initial conditions inside and outside the separatrix is described, the role of vortex-shear interactions being highlighted. Chaotic motion around the separatrix is contrasted with that inside the separatrix and a form of chaotic scattering is detected.

This paper concludes, in Sec. VI, with a brief discussion of the results.

II. HAMILTONIAN MOMENT FORMULATION

In this section, the equations of motion for N elliptical vortices in a background Kida flow are derived following FMM. Using a Hamiltonian moment formulation in which the quadratic vorticity moments are the dynamical variables, FMM were able to derive the equations of motion for the Kida vortex. Our work generalizes that of FMM by extending the analysis to N interacting vortices. Briefly, our derivation proceeds by: (i) expressing the Poisson bracket for the 2-D Euler equations in terms of the first and second order vorticity moments; (ii) determining the cosymplectic matrix J^{jk} from the bracket; (iii) computing the Hamiltonian in terms of the moments; and (iv) obtaining the equations of motion from H and J^{jk}.

A. Poisson bracket

First, let us consider a two-dimensional Euler flow with a spatially and temporally varying vorticity distribution, $q(\boldsymbol{x}, t)$. We make the assumption that q approaches a uniform, constant value, say ω, sufficiently rapidly as $|\boldsymbol{x}| \to \infty$, and we set $q(\boldsymbol{x}, t) = \omega + q'(\boldsymbol{x}, t)$.

The Poisson bracket for two-dimensional Euler flow is[14]

$$\{F, G\} = \int q' \left[\frac{\delta F}{\delta q'}, \frac{\delta G}{\delta q'} \right] dxdy, \tag{6}$$

where F and G are functionals of vorticity, $\delta/\delta q'$ denotes a functional derivative, $[a,b] = a_x b_y - b_x a_y$ is the two-dimensional Jacobian, and the constant background vorticity does not appear. (The background vorticity will enter in the Hamiltonian by virtue of the dynamical role associated with the background flow.) We introduce a finite set of functionals of the perturbation vorticity which we call *moments*, $\{a^j[q'] : j = 0, \ldots, K-1\}$. For a subset of functionals of q' depending only on q' as *functions* of the moments, e.g. $F[q'] = f(a^0[q'], \ldots, a^{K-1}[q'])$,

$$\frac{\delta F}{\delta q'} = \frac{\partial f}{\partial a^j} \frac{\delta a^j}{\delta q'}$$

and (6) takes the form

$$\begin{aligned} \{F, G\} &= \frac{\partial f}{\partial a^j} \frac{\partial g}{\partial a^k} \int q' \left[\frac{\delta a^j}{\delta q'}, \frac{\delta a^k}{\delta q'} \right] dxdy \\ &= \frac{\partial f}{\partial a^j} J^{jk} \frac{\partial g}{\partial a^k} \end{aligned} \tag{7}$$

where

$$J^{jk} = \int q' \left[\frac{\delta a^j}{\delta q'}, \frac{\delta a^k}{\delta q'} \right] dxdy. \tag{8}$$

The success of this approach depends on whether we are able to approximate the Hamiltonian of the system as a function of the moments, $\{a^j\}$. This will in turn depend both on the nature of the scalar field $q'(\boldsymbol{x})$ and on our particular choice of moments.

Let us now move in the direction of *spatial* moments by introducing a finite (but as yet, arbitrary) set of time-dependent disjoint areas $\{S_j(t) : j = 0, \ldots, N-1\}$ and defining the set of moments, $\{\tilde{a}^j\}$, in terms of them by

$$\tilde{a}^j := \int q' \chi_k(\boldsymbol{x}) \chi_l(\boldsymbol{x}) x^r x^s \, dxdy, \tag{9}$$

where r and s are nonnegative integers and $r + s \leq 2$ for $0 \leq k, l \leq N-1$. Here $\chi_j(\boldsymbol{x}) = 1$ if $\boldsymbol{x} \in S_j$ and $\chi_j(\boldsymbol{x}) = 0$ otherwise. The monomials x^r and x^s may be associated with $\chi_k(\boldsymbol{x})$

and $\chi_l(\boldsymbol{x})$, respectively. Provided that q' is such that we can choose the $\{S_j\}$ so that $q' = 0$ on their boundaries, the Jacobians in the integrands of (8) are polynomials of at most second degree. This ensures that J^{jk} takes the form

$$J^{jk} = c_\ell^{jk}\tilde{a}^\ell. \tag{10}$$

From the properties of the Jacobian, $[\,,\,]$, the constants c_ℓ^{jk} inherit the following properties: (a) they are skew-symmetric, $c_\ell^{jk} = -c_\ell^{kj}$; and (b) they satisfy Jacobi's identity, $c_r^{js}c_s^{k\ell}+c_r^{ks}c_s^{\ell j}+c_r^{\ell s}c_s^{jk} = 0$. The c_ℓ^{jk} are therefore the structure constants of a Lie algebra and the bracket, (7), is a Lie-Poisson bracket with cosymplectic matrix J. If the perturbation vorticity field has the form of "clumps," so that q' is nonzero only on a set of compact, disjoint regions, $\{D_i\,:\,i = 0,\ldots,N-1\}$, then we may obtain a further simplification. Choosing the S_i so that each S_i completely contains the corresponding D_i but does not intersect any of the remaining D's, the moments in (9) are zero unless $k = l$—the moments have compact support. Note that because of the vorticity conserving property of the Euler equations, the moments are simply constants for $r = s = 0$.

With these simplifications, we can think of our model as approximating the vorticity distribution by a collection of elliptical patches of uniform vorticity, one patch being assigned to each of the disjoint clumps in the original q' distribution. More formally, there is a simple correspondence between the instantaneous state of the moments and the configuration of a collection of uniform elliptical patches. First order moments determine the positions of the centroids, and second order moments define the aspect ratio and orientation of the equivalent ellipses. Each vortex embodies an infinite number of degrees of freedom corresponding to the shape of each region D_i and the distribution of the vorticity within it. The moment reduction, as we shall see, restricts this number to only two degrees of freedom per vortex, one associated with the vortex centroid, and one with its ellipticity and orientation.

For the specific problem considered in this paper, we adopt the second perspective: N

elliptical patches of uniform vorticity, q_i' $(i = 0, \ldots, N-1)$, each with area, A_i, and circulation, Γ_i. The steady uniform background vorticity is associated with a flow that combines both background rotation and strain:

$$\Psi = \frac{1}{4}\omega(x^2 + y^2) + \frac{1}{4}e(x^2 - y^2), \tag{11}$$

ω and e being constants. This is the same background flow used in the Kida problem.

We now label the moments with a single suffix that combines information about both the polynomial used to generate the moment and the vortex with which it is associated. (To avoid unnecessary confusion, we lower the indices on the a's.) After the reduction sketched above, we find that there are six moments associated with each vortex. One is the circulation of the vortex,

$$\Gamma_i := \tilde{a}_{-3-3i} := \int_{D_i} q_i' \, dxdy; \tag{12}$$

two are the first moments of the vorticity,

$$\tilde{a}_{-1-3i} = \int_{D_i} q_i' x \, dxdy \qquad \tilde{a}_{-2-3i} = \int_{D_i} q_i' y \, dxdy; \tag{13}$$

and the remaining three are second order moments,

$$\begin{aligned} \tilde{a}_{1+3i} &= \int_{D_i} q_i' x^2 \, dxdy \\ \tilde{a}_{2+3i} &= \int_{D_i} q_i' xy \, dxdy \\ \tilde{a}_{3+3i} &= \int_{D_i} q_i' y^2 \, dxdy. \end{aligned} \tag{14}$$

The i's identify the vortices.

It is convenient to define functions $\widetilde{m}_j$ associated with the integrands of the $\tilde{a}_j$:

$$\widetilde{m}_{1+3i} = x^2, \qquad \widetilde{m}_{2+3i} = xy, \qquad \widetilde{m}_{3+3i} = y^2, \tag{15}$$

$$\widetilde{m}_{-1-3i} = x, \qquad \widetilde{m}_{-2-3i} = y, \qquad \widetilde{m}_{-3-3i} = 1.$$

The structure constants c_ℓ^{jk} can then be evaluated from the relations

$$[\widetilde{m}_{1+3i},\ \widetilde{m}_{3+3i}] = 4\widetilde{m}_{2+3i}, \qquad [\widetilde{m}_{1+3i},\ \widetilde{m}_{2+3i}] = 2\widetilde{m}_{1+3i}, \tag{16}$$

$$[\widetilde{m}_{2+3i},\ \widetilde{m}_{3+3i}] = 2\widetilde{m}_{3+3i}, \qquad [\widetilde{m}_{-1-3i},\ \widetilde{m}_{-2-3i}] = 1,$$

$$[\widetilde{m}_{-1-3i},\ \widetilde{m}_{1+3i}] = 0, \qquad [\widetilde{m}_{-2-3i},\ \widetilde{m}_{3+3i}] = 0,$$

and

$$[\widetilde{m}_{-1-3i}, \widetilde{m}_{2+3i}] = \widetilde{m}_{-1-3i}, \qquad [\widetilde{m}_{-1-3i}, \widetilde{m}_{3+3i}] = 2\widetilde{m}_{-2-3i}, \tag{17}$$

$$[\widetilde{m}_{-2-3i}, \widetilde{m}_{1+3i}] = -2\widetilde{m}_{-1-3i}, \qquad [\widetilde{m}_{-2-3i}, \widetilde{m}_{2+3i}] = -\widetilde{m}_{-2-3i}.$$

(Any Jacobian with $\widetilde{m}_{-3-3i}$ as one of its arguments is clearly zero.)

B. Cosymplectic matrix

The cosymplectic matrix $\tilde{J}^{jk}$ is defined by

$$\{F, G\} = \frac{\partial F}{\partial \widetilde{a}_j}\, \tilde{J}^{jk}\, \frac{\partial G}{\partial \widetilde{a}_k}. \tag{18}$$

From (8), we see that

$$\tilde{J}^{jk} = \int q_j' \, [\widetilde{m}_j, \widetilde{m}_k]\, \chi_j \chi_k dx dy. \tag{19}$$

By construction, (19) is antisymmetric and guarantees that (18) satisfies Jacobi's identity: an existing Poisson bracket has been reduced using variables that constitute a Lie subalgebra.[14] (Note that $\delta\widetilde{a}_j/\delta q_j' = \widetilde{m}_j\chi_j$.)

Because of the factor of $\chi_j\chi_k$ in the preceding expression, moments of different vortices do not couple together. It follows from the products (16)–(17) and the definitions of $\widetilde{a}_j$ that $\tilde{J}$ is a direct sum over $\tilde{J}_i$, the single-vortex cosymplectic matrices:

$$\tilde{J} = \bigoplus_{i=0}^{N-1} \tilde{J}_i. \tag{20}$$

For $N = 2$ vortices, J takes the block-diagonal form

$$\tilde{J} = \begin{pmatrix} \tilde{J}_0 & 0 \\ 0 & \tilde{J}_1 \end{pmatrix}. \tag{21}$$

Ordering the variables as $(z_1 \ldots z_{6N})$ where

$$(z_{1+6i}, z_{2+6i}, z_{3+6i}, z_{4+6i}, z_{5+6i}, z_{6+6i}) = (\tilde{a}_{-3-3i},\ \tilde{a}_{-1-2i},\ \tilde{a}_{-2-2i},\ \tilde{a}_{1+3i},\ \tilde{a}_{2+3i},\ \tilde{a}_{3+3i}),$$

$\tilde{J}_i$, a 6×6 matrix, has the following structure:

$$\tilde{J}_i = \begin{pmatrix} 0 & 0 & 0 \\ 0 & \mathcal{A}_i & \mathcal{C}_i \\ 0 & -\mathcal{C}_i^T & \mathcal{B}_i \end{pmatrix}, \tag{22}$$

with

$$\mathcal{A}_i = \begin{pmatrix} 0 & \tilde{a}_{-3-3i} \\ -\tilde{a}_{-3-3i} & 0 \end{pmatrix}, \tag{23}$$

$$\mathcal{B}_i = \begin{pmatrix} 0 & 2\tilde{a}_{1+3i} & 4\tilde{a}_{2+3i} \\ -2\tilde{a}_{1+3i} & 0 & 2\tilde{a}_{3+3i} \\ -4\tilde{a}_{2+3i} & -2\tilde{a}_{3+3i} & 0 \end{pmatrix}, \tag{24}$$

and

$$\mathcal{C}_i = \begin{pmatrix} 0 & \tilde{a}_{-1-3i} & 2\tilde{a}_{-2-3i} \\ -2\tilde{a}_{-1-3i} & -\tilde{a}_{-2-3i} & 0 \end{pmatrix}. \tag{25}$$

Before turning to the Hamiltonian, we first note that the system has some symmetries that are independent of the form of the Hamiltonian. These symmetries are manifested in Casimir invariants C, which are solutions of

$$0 = J^{jk} \frac{\partial C}{\partial z^k}. \tag{26}$$

The Casimirs arise when the cosymplectic matrix is singular and correspond to constants of the motion. There are infinitely many Casimirs for the 2-D Euler equations, the materially conserved functionals of vorticity, but only $2N$ Casimirs for a system of N elliptical vortices

in shear. Given the zeroes in the first column and row of $\tilde{J}$, the net circulation of each vortex, $\tilde{a}_{-3-3i}$, is clearly a Casimir.

Change of coordinates

Since one of the coordinates in (22) is a Casimir, we can treat it as a constant parameter and reduce the dimension of the submatrices $\tilde{J}_i$ by one. This leaves five remaining variables per vortex, $\tilde{a}_{-1-3i}$, $\tilde{a}_{-2-3i}$, $\tilde{a}_{1+3i}$, $\tilde{a}_{2+3i}$, and $\tilde{a}_{3+3i}$. The submatrices can themselves be rendered block diagonal by using a transformation that replaces the second order moments with second order moments *about the vortex centroid.* We set

$$a_{-j-3i} = \tilde{a}_{-j-3i} \tag{27}$$

$$x_i^* = a_{-1-3i}/a_{-3-3i}, \qquad y_i^* = a_{-2-3i}/a_{-3-3i}$$

$$a_{1+3i} = \tilde{a}_{1+3i} - x_i^{*2} a_{-3-3i}, \tag{28}$$

$$a_{2+3i} = \tilde{a}_{2+3i} - x_i^* y_i^* a_{-3-3i},$$

$$a_{3+3i} = \tilde{a}_{3+3i} - y_i^{*2} a_{-3-3i}.$$

The variables (x_i^*, y_i^*) are just the coordinates of the centroid of the i th vortex. In the new coordinates $\{a_j\}$, we denote the cosymplectic matrix by J^{jk}. After defining new functions m_j, the mixed products corresponding to (17) vanish when integrated over D_i because

$$\int_{D_i} q_i'(x - x_i^*) = \int_{D_i} q_i'(y - y_i^*) = 0.$$

The elements of the submatrix $\mathcal{C}_i$ are thus identically zero and the new cosymplectic matrix takes the form

$$J = \bigoplus_{i=1}^{N} J_i; \qquad J_i = \begin{pmatrix} \mathcal{A}_i & 0 \\ 0 & \mathcal{B}_i \end{pmatrix}. \tag{29}$$

The block diagonal submatrices $\mathcal{A}_i$, $\mathcal{B}_i$ are given by (23) and (24), the $\tilde{a}$'s being replaced by a's. $\mathcal{A}_i$ is, to within a normalization factor, the canonical cosymplectic matrix for point

vortex motion; $\mathcal{B}_i$ is the cosymplectic matrix for a Kida vortex (cf. FMM). The block diagonal form of $\tilde{J}$ shows that, in this coordinate system, the vortices are not coupled through the cosymplectic matrix. Coupling between the vortices arises through the Hamiltonian.

The existence of a second Casimir for each vortex now becomes apparent since (26) also has the solution

$$C^i = a_{1+3i}a_{3+3i} - a_{2+3i}^2. \tag{30}$$

For the particular case of uniform elliptical vortices, this is again related to the circulation of an individual vortex:

$$C^i = \frac{\Gamma_i^2 A_i^2}{16\pi^2}. \tag{31}$$

This is not true in the general case, however (cf. FMM).

C. Hamiltonian

We now seek an approximation to the Hamiltonian written wholly in terms of the $\tilde{a}_j$. For the 2-D Euler equations, the excess energy is an invariant quantity.[27] For a system of N uniform vortices in an unbounded domain with a background flow Ψ of uniform vorticity, the excess energy is

$$E = -\frac{1}{2}\sum_{j=0}^{N-1}\int_{D_j}(2\Psi + \sum_{i=1}^{N}\psi_i')q_j'\,d\boldsymbol{x}$$

where ψ_i' is the streamfunction induced by vortex i. For point vortex motion, the excess energy is the Hamiltonian. With the ansatz that the excess energy is the Hamiltonian for our system, we obtain

$$H = -\frac{1}{2}\sum_{i=0}^{N-1}\left\{\int_{D_i} 2\Psi q_i'\,dxdy + \int_{D_i}\psi_i' q_i'\,dxdy + \sum_{j=0}^{N-1}{}'\int_{D_i}\psi_j' q_i'\,dxdy\right\}, \tag{32}$$

or

$$H = H_1 + H_2 + H_3,$$

respectively. The first term in (32) corresponds to interactions of the background flow with the vortices, the second to interactions of the vortices with themselves, and the third to interactions of the vortices with one another. (The notation $\sum_{j=0}^{N-1}{}'$ stands for $\sum_{j=0,j\neq i}^{N-1}$.)

The contribution to the streamfunction induced by a patch, D_i, of vorticity, q_i', is

$$\psi_i'(\boldsymbol{x}) = \int_{D_i} q_i' \, G(\boldsymbol{x}, \boldsymbol{x}') \, dx'dy' \tag{33}$$

where

$$G(\boldsymbol{x}, \boldsymbol{x}') = \frac{1}{2\pi} \ln \mid \boldsymbol{x} - \boldsymbol{x}' \mid .$$

We now compute the three terms in (32). The first term can be written as

$$H_1 = -\sum_{i=0}^{N-1} \int_{D_i} q_i' \left[\frac{1}{4}(\omega + e)x^2 + \frac{1}{4}(\omega - e)y^2 \right] dxdy \tag{34}$$

$$= -\sum_{i=0}^{N-1} \left\{ \frac{1}{4}(\omega + e) \left[a_{1+3i} + \frac{a_{-1-3i}^2}{a_{-3-3i}} \right] + \frac{1}{4}(\omega - e) \left[a_{3+3i} + \frac{a_{-2-3i}^2}{a_{-3-3i}} \right] \right\}.$$

So far we have not made any approximations. We now introduce two approximations that allow us to estimate H_2 and H_3. *(a)* We make the approximation that the vortices are close to elliptical in shape with close to uniform vorticity. The existence of the circulation Casimir then implies conservation of individual vortex area. A constant area ellipse can be characterized by four parameters, for example, its aspect ratio, λ (the ratio of the semi-major and semi-minor axes), its orientation, ϕ (the angle between the fixed coordinate axes and the rotating body frame), and the x and y centroids. These four parameters are uniquely determined by the first and second order spatial moments of the ellipse. The centroid coordinates have already been discussed; the second order moments are related to the aspect ratio and orientation by

$$a_{1+3i} = \left(\lambda_i^{-1} \cos^2 \phi_i + \lambda_i \sin^2 \phi_i \right) \frac{\Gamma_i A_i}{4\pi} \tag{35}$$

$$a_{2+3i} = \left(\lambda_i^{-1} - \lambda_i \right) \sin \phi_i \cos \phi_i \frac{\Gamma_i A_i}{4\pi}$$

$$a_{3+3i} = \left(\lambda_i^{-1}\sin^2\phi_i + \lambda_i\cos^2\phi_i\right)\frac{\Gamma_i A_i}{4\pi}.$$

(b) Our second approximation is that the vortices remain well separated in the sense that the vortex separations R_{ij} and the length scales of the vortices, characterized by the length of their semi-major axes, b_i, satisfy

$$\varepsilon_{ij} := \frac{b_i}{R_{ij}} \ll 1. \tag{36}$$

To evaluate the term H_2, we only need the first approximation, that the vortices are nearly elliptical. Using (33), H_2 can be written as

$$H_2 = -\frac{1}{2}\sum_{i=0}^{N-1} q_i'^2 \int_{D_i} d\boldsymbol{x}_i \int_{D_i} d\boldsymbol{x}_i' G(\boldsymbol{x},\boldsymbol{x}'). \tag{37}$$

Assuming that D_i is an ellipse with aspect ratio λ_i this becomes

$$H_2 = -\frac{1}{8\pi}\sum_{i=0}^{N-1} \Gamma_i^2 \ln\frac{(1+\lambda_i)^2}{\lambda_i};$$

and from (35),

$$H_2 = -\frac{1}{8\pi}\sum_{i=0}^{N-1} \Gamma_i^2 \ln\left[(a_{1+3i}+a_{3+3i})\frac{4\pi}{\Gamma_i A_i}+2\right]. \tag{38}$$

The final term, H_3, may be written

$$H_3 = -\frac{1}{4\pi}\sum_{i=0}^{N-1}\sum_{j=0}^{N-1}{}' \; q_i' q_j' \int_{D_i} d\boldsymbol{x}_i \int_{D_j} d\boldsymbol{x}_j \ln\mid \boldsymbol{x}_i - \boldsymbol{x}_j' \mid. \tag{39}$$

Letting $\boldsymbol{x}_i = \boldsymbol{R}_i + \tilde{\boldsymbol{x}}_i$ where $\boldsymbol{R}_i = (x_i^*, y_i^*)$, we obtain

$$H_3 = -\frac{1}{4\pi}\sum_{i=0}^{N-1}\sum_{j=0}^{N-1}{}' q_i' q_j' \int_{D_i} d\tilde{\boldsymbol{x}}_i \int_{D_j} d\tilde{\boldsymbol{x}}_j \ln\mid (\boldsymbol{R}_i+\tilde{\boldsymbol{x}}_i) - (\boldsymbol{R}_j+\tilde{\boldsymbol{x}}_j)\mid.$$

After dropping the tildes, and defining $\boldsymbol{R}_{ij} = \boldsymbol{R}_i - \boldsymbol{R}_j$,

$$H_3 = -\frac{1}{8\pi}\sum_{i=0}^{N-1}\sum_{j=0}^{N-1}{}' q_i' q_j' \int_{D_i} d\boldsymbol{x}_i \int_{D_j} d\boldsymbol{x}_j \Bigg\{ \ln R_{ij}^2$$

$$+ \ln\left[1 + \frac{\boldsymbol{R}_{ij}\cdot(\boldsymbol{x}_i-\boldsymbol{x}_j)}{R_{ij}^2} + \frac{|\boldsymbol{x}_i-\boldsymbol{x}_j|^2}{R_{ij}^2}\right]\Bigg\}.$$

We use the second approximation, (36), to expand the second logarithmic term and truncate at second order in ε_i. The result is an expression involving only zeroth, first and second order moments:

$$H_3 = -\frac{1}{8\pi} \sum_{i=0}^{N-1} {\sum_{j=0}^{N-1}}' \Bigg\{ \Gamma_i \Gamma_j \ln R_{ij}^2 + \frac{2}{R_{ij}^2} \Bigg[\frac{1}{2} \Gamma_i (a_{1+3j} + a_{3+3j}) + \frac{1}{2} \Gamma_j (a_{1+3i} + a_{3+3i}) \\ - \cos^2 \theta_{ij} (\Gamma_i a_{1+3j} + \Gamma_j a_{1+3i}) - \sin^2 \theta_{ij} (\Gamma_i a_{3+3j} + \Gamma_j a_{3+3i}) \\ - \sin 2\theta_{ij} (\Gamma_i a_{2+3j} + \Gamma_j a_{2+3i}) \Bigg] \Bigg\}, \tag{40}$$

where

$$(R_{ij} \cos \theta_{ij}, R_{ij} \sin \theta_{ij}) = \left(x_i^* - x_j^*, y_i^* - y_j^* \right). \tag{41}$$

Combining terms,

$$H = -\frac{1}{4} \sum_{i=0}^{N-1} \Bigg\{ \left[(\omega + e) a_{1+3i} + (\omega - e) a_{3+3i} + (\omega + e) \frac{a_{-1-3i}^2}{\Gamma_i} + (\omega - e) \frac{a_{-2-3i}^2}{\Gamma_i} \right] \\ + \frac{\Gamma_i^2}{2\pi} \ln \left\{ \left[(a_{1+3i} + a_{3+3i}) \frac{4\pi}{\Gamma_i A_i} + 2 \right] \right\} \\ + \frac{1}{2\pi} {\sum_{j=0}^{N-1}}' \left[\Gamma_i \Gamma_j \ln R_{ij}^2 + \frac{2}{R_{ij}^2} (\alpha_{ij} \cos 2\theta_{ij} - 2\beta_{ij} \sin 2\theta_{ij}) \right] \Bigg\}, \tag{42}$$

where

$$\alpha_{ij} = \Gamma_i \left(a_{3+3j} - a_{1+3j} \right)$$

$$\beta_{ij} = \Gamma_i a_{2+3j}.$$

Like the cosymplectic matrix, the Hamiltonian possesses several symmetries. There is a decoupling between the first and second order moments. The Hamiltonian is invariant under a change of vortex labels; the interaction energy of vortex i with vortex j is, as it must be, the same as that of vortex j with vortex i. A fact we shall use later is that the Hamiltonian

may be decomposed into a part which depends only on global centroid information and a part which depends only on the vortices' relative displacement.

For $N = 2$ vortices, we let $R = R_{ij} = R_{ji}$ and $\theta = \theta_{ij} = -(\pi - \theta_{ji})$. The Hamiltonian is given by

$$\begin{aligned} H = & -\frac{1}{4}\left[(\omega+e)a_1 + (\omega-e)a_3 + (\omega+e)\frac{a_{-1}^2}{\Gamma_0} + (\omega-e)\frac{a_{-2}^2}{\Gamma_0}\right] \\ & -\frac{1}{4}\left[(\omega+e)a_4 + (\omega-e)a_6 + (\omega+e)\frac{a_{-4}^2}{\Gamma_1} + (\omega-e)\frac{a_{-5}^2}{\Gamma_1}\right] \\ & -\frac{\Gamma_0^2}{8\pi}\ln\left[(a_1+a_3)\frac{4\pi}{\Gamma_0 A_0} + 2\right] - \frac{\Gamma_1^2}{8\pi}\ln\left[(a_4+a_6)\frac{4\pi}{\Gamma_1 A_1} + 2\right] \\ & -\frac{1}{4\pi}\Bigg[\Gamma_0\Gamma_1 \ln R^2 \\ & \qquad +\frac{1}{R^2}\Big\{\cos 2\theta\left[\Gamma_0(a_6-a_4) + \Gamma_1(a_3-a_1)\right] - 2\sin 2\theta\left[\Gamma_0 a_5 + \Gamma_1 a_2\right]\Big\}\Bigg]. \end{aligned} \tag{43}$$

D. Equations of motion for a_i

We now compute the equations of motion from (5) and (22)–(24), i.e. from

$$\begin{aligned} \dot{a}_{1+3i} &= 2a_{1+3i}\frac{\partial H}{\partial a_{2+3i}} + 4a_{2+3i}\frac{\partial H}{\partial a_{3+3i}} \\ \dot{a}_{2+3i} &= -2a_{1+3i}\frac{\partial H}{\partial a_{1+3i}} + 2a_{3+3i}\frac{\partial H}{\partial a_{3+3i}} \\ \dot{a}_{3+3i} &= -4a_{2+3i}\frac{\partial H}{\partial a_{1+3i}} - 2a_{3+3i}\frac{\partial H}{\partial a_{2+3i}}, \end{aligned}$$

and

$$\dot{a}_{-1-3i} = \Gamma_i\frac{\partial H}{\partial a_{-2-3i}} \qquad \dot{a}_{-2-3i} = -\Gamma_i\frac{\partial H}{\partial a_{-1-3i}}.$$

The equations of motion for the quadratic moments are

$$\dot{a}_{1+3i} = \sum_{j=0}^{N-1}{}' \frac{a_{1+3i}\,\Gamma_j \sin 2\theta_{ij}}{\pi R_{ij}^2} \tag{44}$$

$$+a_{2+3i}\left[-(\omega-e)-\frac{2q_i'}{[(a_{1+3i}+a_{3+3i})\frac{4\pi}{\Gamma_i A_i}+2]}-\sum_{j=0}^{N-1}{}'\frac{\Gamma_j\cos 2\theta_{ij}}{\pi R_{ij}^2}\right]$$

$$\dot{a}_{2+3i}=\frac{1}{2}\,\omega(a_{1+3i}-a_{3+3i})+\frac{1}{2}\,e(a_{1+3i}+a_{3+3i})$$

$$+q_i'\frac{(a_{1+3i}-a_{3+3i})}{[(a_{1+3i}+a_{3+3i})\frac{4\pi}{\Gamma_i A_i}+2]}-\sum_{j=0}^{N-1}{}'\frac{\Gamma_j\cos 2\theta_{ij}}{2\pi R_{ij}^2}\,(a_{1+3i}+a_{3+3i})$$

$$\dot{a}_{3+3i}=\sum_{j=0}^{N-1}{}'-\frac{a_{3+3i}\Gamma_j\sin 2\theta_{ij}}{\pi R_{ij}^2}$$

$$+a_{2+3i}\left[(\omega+e)+\frac{2q_i'}{[(a_{1+3i}+a_{3+3i})\frac{4\pi}{\Gamma_i A_i}+2]}-\sum_{j=0}^{N-1}{}'\frac{\Gamma_j\cos 2\theta_{ij}}{\pi R_{ij}^2}\right].$$

After some simplification, the first order equations are

$$\dot{x}_i^*=-\frac{1}{2}\,(\omega-e)y_i^*-\sum_{j=0}^{N-1}{}'\frac{\Gamma_j}{2\pi R_{ij}}\sin\theta_{ij} \tag{45}$$

$$+\frac{1}{\Gamma_i}\sum_{j=0}^{N-1}{}'\frac{1}{2\pi R_{ij}^3}\left\{(\alpha_{ij}+\alpha_{ji})\sin 3\theta_{ij}+2(\beta_{ij}+\beta_{ji})\cos 3\theta_{ij}\right\}$$

$$\dot{y}_i^*=\frac{1}{2}\,(\omega+e)x_i^*+\sum_{j=0}^{N-1}{}'\frac{\Gamma_j}{2\pi R_{ij}}\cos\theta_{ij}$$

$$+\frac{1}{\Gamma_i}\sum_{j=0}^{N-1}{}'\frac{1}{2\pi R_{ij}^3}\left\{-(\alpha_{ij}+\alpha_{ji})\cos 3\theta_{ij}+2(\beta_{ij}+\beta_{ji})\sin 3\theta_{ij}\right\}.$$

The equations (44) and (45) constitute a set of $5N$ coupled ODE's. They are a closed set even though they do not contain explicit evolution equations for R_{ij} and θ_{ij} because R_{ij} and θ_{ij} may be determined from (41).

The equations can be simplified in the following way. Since the N quantities $C^i = a_{1+3i}a_{3+3i}-a_{2+3i}^2$ are Casimirs, a_{1+3i}, a_{2+3i}, and a_{3+3i} are not all independent of one another. This can be made explicit by employing a transformation of variables wherein the Casimirs act as dependent variables, thereby leaving a set of only $4N$ independent equations of motion

(N equations reduce to $dC^i/dt = 0$). A further simplification may be had by noting that the equations of motion do not depend on the global centroid position; one is left with a system of $4N - 2$ equations after appropriate linear combinations are taken. (Formally, this set is generated by decoupling the global centroid from the Hamiltonian (42).)

E. Equations of motion in physical variables

By transforming to the more intuitive variables, $(x_i^*, y_i^*, \lambda_i, \phi_i)$, a set of equations analogous to those of MZS is obtained.

The equations for the evolution of (x_i^*, y_i^*) are (45). Using (35), we find that λ_i and ϕ_i evolve according to

$$\dot{\lambda}_i = -\lambda_i \sum_{j=0}^{N-1}{}' \left[\frac{\Gamma_j}{\pi R_{ij}^2} \sin 2(\theta_{ij} - \phi_i) + e \sin 2\phi_i \right] \tag{46}$$

$$\dot{\phi}_i = \frac{q_i' \lambda_i}{(1+\lambda_i)^2} - \frac{1}{2} \frac{1+\lambda_i^2}{1-\lambda_i^2} \left\{ \frac{\Gamma_j}{\pi R_{ij}^2} \cos 2(\theta_{ij} - \phi_i) - e \cos 2\phi_i \right\} + \frac{\omega}{2}.$$

In the $\dot{\phi}_i$ equation, there is an apparent singularity when $\lambda_i = 1$. As noted by MZS, this singularity arises from the fact that the orientation of a circular vortex is not well-defined. MZS point out that one way to "desingularize" these equations is to introduce new variables

$$(\delta_i, \gamma_i) = \left(\frac{A_i}{8\pi\lambda_i} \right)^{\frac{1}{2}} (\lambda_i - 1)(\cos 2\phi_i, \sin 2\phi_i).$$

MZS further note that $((\lambda_i - 1)^{2/\lambda_i},\ 2\phi_i)$ is one set canonical variables for this problem. This set was later used by Ide and Wiggins (1995)[42] in a study of the motion of a single elliptical vortex in a time-dependent linear background flow; an alternative set is introduced in FMM. Nevertheless, there is an essential singularity at $R_{ij} = 0$ which cannot be removed by a coordinate transformation. Following MZS we take $R_{ij} \to 0$ as being indicative of vortex merger, but it should be noted that the model ceases to be consistent in this limit because the assumption of well-separated vortices breaks down.

F. Equations of motion for $N = 2$

It is useful to present the equations of motion for $N = 2$ vortices in one place.

In terms of aspect ratios and orientations, the equations take the form:

$$\dot{R} = \frac{1}{2} eR \sin 2\theta - \frac{\Gamma_0 + \Gamma_1}{8\pi^2 R^3} \left\{ A_0 \frac{1-\lambda_0^2}{\lambda_0} \sin 2(\theta - \phi_0) + A_1 \frac{1-\lambda_1^2}{\lambda_1} \sin 2(\theta - \phi_1) \right\} \tag{47}$$

$$\dot{\theta} = \frac{\omega}{2} + \frac{e}{2} \cos 2\theta + \frac{\Gamma_0 + \Gamma_1}{2\pi R^2}$$

$$+ \frac{\Gamma_0 + \Gamma_1}{8\pi^2 R^4} \left\{ A_0 \frac{1-\lambda_0^2}{\lambda_0} \cos 2(\theta - \phi_0) + A_1 \frac{1-\lambda_1^2}{\lambda_1} \cos 2(\theta - \phi_1) \right\}$$

$$\dot{\lambda}_0 = -\lambda_0 \left\{ \frac{\Gamma_1}{\pi R^2} \sin 2(\theta - \phi_0) + e \sin 2\phi_0 \right]$$

$$\dot{\lambda}_1 = -\lambda_1 \left\{ \frac{\Gamma_0}{\pi R^2} \sin 2(\theta - \phi_1) + e \sin 2\phi_1 \right]$$

$$\dot{\phi}_0 = \frac{q_0' \lambda_0}{(1+\lambda_0)^2} - \frac{1}{2} \frac{1+\lambda_0^2}{1-\lambda_0^2} \left\{ \frac{\Gamma_1}{\pi R^2} \cos 2(\theta - \phi_0) - e \cos 2\phi_0 \right\} + \frac{\omega}{2}$$

$$\dot{\phi}_1 = \frac{q_1' \lambda_1}{(1+\lambda_1)^2} - \frac{1}{2} \frac{1+\lambda_1^2}{1-\lambda_1^2} \left\{ \frac{\Gamma_0}{\pi R^2} \cos 2(\theta - \phi_1) - e \cos 2\phi_1 \right\} + \frac{\omega}{2};$$

and the Hamiltonian is given by

$$-4\pi H = \Gamma_0 \Gamma_1 \ln R^2 + \frac{1}{2} \left\{ \Gamma_0^2 \ln \frac{(1+\lambda_0)^2}{\lambda_0} + \Gamma_1^2 \ln \frac{(1+\lambda_1)^2}{\lambda_1} \right\} \tag{48}$$

$$+ \frac{\Gamma_0 + \Gamma_1}{4} \pi R^2 (\omega + e \cos 2\theta)$$

$$+ \frac{\Gamma_0 A_0}{4} \left[\omega(\lambda_0 + \lambda_0^{-1}) + e(\lambda_0^{-1} - \lambda_0) \cos 2\phi_0 \right]$$

$$+ \frac{\Gamma_1 A_1}{4} \left[\omega(\lambda_1 + \lambda_1^{-1}) + e(\lambda_1^{-1} - \lambda_1) \cos 2\phi_1 \right]$$

$$+ \frac{\Gamma_0 \Gamma_1}{4\pi R^2} \left[A_0(\lambda_0 - \lambda_0^{-1}) \cos 2(\theta - \phi_0) + A_1(\lambda_1 - \lambda_1^{-1}) \cos 2(\theta - \phi_1) \right].$$

III. BASIC ANALYSIS

In this section, we begin the analysis of our model. We use the formulation in aspect ratio–orientation variables because physical processes are discerned more easily within it. We will soon restrict ourselves to a system of two identical vortices. While more complicated configurations will, or course, exhibit behavior which a symmetric vortex pair cannot, the vortex-vortex and vortex-shear interactions that we analyze below are still present in more complicated configurations—there are just more of them. The Hamiltonian for N vortices (42) is not fundamentally different from that for two vortices (43): there are no multipole interactions at the order of our truncation.

A. Nondimensionalization

Our starting point is the system (47). Letting D denote a characteristic separation scale, we nondimensionalize as follows. We set $R = rD$, $e = \tilde{e}q_0$, $\omega = \alpha\tilde{e}q_0$, $\delta = A_1/A_0$, $\nu = q_1/q_0$, and scale time by q_0^{-1}. We define a nondimensional perturbation parameter

$$\epsilon = \frac{A_0}{\pi D^2}, \tag{49}$$

which we assume to be small. Then (47) becomes

$$\dot{r} = \frac{1}{2}\tilde{e}r\sin 2\theta - \epsilon^2\frac{1+\delta\nu}{8r^3}\left\{\frac{1-\lambda_0^2}{\lambda_0}\sin 2(\theta-\phi_0) + \delta\frac{1-\lambda_1^2}{\lambda_1}\sin 2(\theta-\phi_1)\right\} \tag{50}$$

$$\dot{\theta} = \frac{\tilde{e}}{2}(\alpha+\cos 2\theta) + \epsilon\frac{1+\delta\nu}{2r^2} + \epsilon^2\frac{1+\delta\nu}{8r^4}\left\{\frac{1-\lambda_0^2}{\lambda_0}\cos 2(\theta-\phi_0) + \delta\frac{1-\lambda_1^2}{\lambda_1}\cos 2(\theta-\phi_1)\right\}$$

$$\dot{\lambda}_0 = -\lambda_0\left\{\tilde{e}\sin 2\phi_0 + \frac{\epsilon}{r^2}\delta\nu\sin 2(\theta-\phi_0)\right\}$$

$$\dot{\lambda}_1 = -\lambda_1\left\{\tilde{e}\sin 2\phi_1 + \frac{\epsilon}{r^2}\sin 2(\theta-\phi_1)\right\}$$

$$\dot{\phi}_0 = \frac{\lambda_0}{(1+\lambda_0)^2} + \frac{1}{2}\frac{1+\lambda_0^2}{1-\lambda_0^2}\left\{\tilde{e}\cos 2\phi_0 - \delta\nu\frac{\epsilon}{r^2}\cos 2(\theta-\phi_0)\right\} + \alpha\frac{\tilde{e}}{2}$$

$$\dot{\phi}_1 = \frac{\nu\lambda_1}{(1+\lambda_1)^2} + \frac{1}{2}\frac{1+\lambda_1^2}{1-\lambda_1^2}\left\{\tilde{e}\cos 2\phi_1 - \frac{\epsilon}{r^2}\cos 2(\theta-\phi_1)\right\} + \alpha\frac{\tilde{e}}{2}.$$

The terms in (50) have a simple physical interpretation. The terms at $O(1)$ represent (a) the self-rotation of the vortices (the first terms in each of the ϕ equations), and (b) the effects of the background flow on the vortices (the terms involving $\tilde{e}$ in each equation). At $O(\epsilon)$, interactions between the vortices modify the evolution of the aspect ratios and orientations, but have little effect on the separation. They, as with point vortices, produce a constant change in the rotation rate of the separation vector, but no change in its length. At $O(\epsilon^2)$, the shape and separation of the vortices are tightly coupled.

The first two equations in (50), the pair that govern the separation of the vortices, have terms up to $O(\epsilon^2)$, while the remaining four have terms to $O(\epsilon)$. The truncation implicit in (50) arises from the truncation of the Hamiltonian: an infinite moment hierarchy is closed at second order by approximating the vortices as ellipses.

We now specialize to the symmetric case of a pair of identical vortices and set $\lambda = \lambda_0 = \lambda_1$, $\phi = \phi_0 = \phi_1$ and $u = r^2$. As a consequence, $\nu = 1$, $\delta = 1$, and (50) becomes

$$\dot{u} = \tilde{e}u\sin 2\theta - \epsilon^2 u^{-1}\frac{1-\lambda^2}{\lambda}\sin 2(\theta-\phi) \tag{51}$$

$$\dot{\theta} = \frac{\tilde{e}}{2}(\alpha+\cos 2\theta) + \epsilon u^{-1} + \epsilon^2\frac{1}{2}u^{-2}\frac{1-\lambda^2}{\lambda}\cos 2(\theta-\phi)$$

$$\dot{\lambda} = -\lambda\left\{\tilde{e}\sin 2\phi + \epsilon u^{-1}\sin 2(\theta-\phi)\right\}$$

$$\dot{\phi} = \frac{\lambda}{(1+\lambda)^2} + \frac{1}{2}\frac{1+\lambda^2}{1-\lambda^2}\left\{\tilde{e}\cos 2\phi - \epsilon u^{-1}\cos 2(\theta-\phi)\right\} + \alpha\frac{\tilde{e}}{2}.$$

B. Integrable basic states: perturbed point vortex pair in shear

The system (51) is a 4th order (2 degree-of-freedom), nonlinear, Hamiltonian system. In the absence of shear, the 2-D Euler equations conserve angular impulse and the x and y centroids; this leads to two independent integrals of motion for nonvanishing total circulation.[28] These integrals of motion are destroyed by background shear and the Hamiltonian is the only one which remains. From our derivation, we know that this is a Hamiltonian system represented in noncanonical coordinates (see FMM for a discussion of canonical coordinates); we anticipate that there will be chaotic motion because the number of degrees of freedom exceeds the number of integrals of motion.[29] It is possible for points to wander unpredictably over finite regions of phase space because there are fewer integrals of motion than degrees of freedom.

The system (51) can be regarded as a perturbation to any of three integrable basic states: (i) a pair of isolated Kida vortices; (ii) a point vortex pair in shear; and (iii) the MZS model. The equations of motion for a Kida vortex are

$$\dot{\lambda} = -e\lambda \sin 2\phi$$

$$\dot{\phi} = \frac{\lambda}{(1+\lambda)^2} + \frac{\omega}{2} + \frac{1}{2}\frac{1+\lambda^2}{1-\lambda^2} e \cos 2\phi,$$

and the λ and ϕ equations in (51) take this form when $\epsilon = 0$. The (dimensional) equations describing a point vortex pair in shear are

$$\dot{u} = eu \sin 2\theta$$

$$\dot{\theta} = \frac{\omega}{2} + \frac{e}{2} \cos 2\theta + \frac{\Gamma_1 + \Gamma_2}{2\pi u},$$

and correspond to the u and θ equations in (51) when terms in ϵ^2 are neglected. The equations for the MZS model are obtained by setting $\tilde{e} = 0$ in (50). The perturbations to

these basic states then represent the addition of: (i) vortex-vortex interactions; (ii) internal degrees of freedom (aspect ratio and orientation); and (iii) vortex-shear interactions.

We choose to regard (51) as a perturbed point vortex pair in shear. There are two reasons for this choice. The phase space geometry of a point vortex pair in shear provides a particularly convenient framework for studying vortex merger. For sufficiently strong strain, a separatrix divides closed orbits from unbounded ones in the absence of a perturbation (see the Appendix for details). When perturbed, we will find that the vortices can merge and that some of the closed orbits will disappear; furthermore, the separatrix splits apart into distinct stable and unstable manifolds. (The connection between these phenomena is discussed in Sec. 5.) The second reason is a practical one: there exist analytical tools, namely the Melnikov function, which may be applied to systems with heteroclinic orbits.

In preparation for the Melnikov analysis, we apply one more scaling. We are particularly interested in what happens in the vicinity of the separatrix of the point vortex pair. It will prove convenient if the distance from the separatrix to the origin, determined by balancing the first two terms in the θ equation of (51), is scaled to be $O(1)$. This is equivalent to choosing $\tilde{e} = \epsilon\gamma$ where $\gamma = O(1)$. The equations (51) then become,

$$\dot{u} = \epsilon\gamma u \sin 2\theta - \epsilon^2 u^{-1} \frac{1-\lambda^2}{\lambda} \sin 2(\theta - \phi) + O(\epsilon^4) \tag{52}$$

$$\dot{\theta} = \epsilon \left\{ \frac{\gamma}{2} (\alpha + \cos 2\theta) + u^{-1} \right\} + \epsilon^2 \frac{1}{2} u^{-2} \frac{1-\lambda^2}{\lambda} \cos 2(\theta - \phi) + O(\epsilon^4)$$

$$\dot{\lambda} = -\epsilon\lambda \left\{ \gamma \sin 2\phi + u^{-1} \sin 2(\theta - \phi) \right\} + O(\epsilon^3)$$

$$\dot{\phi} = \frac{\lambda}{(1+\lambda)^2} + \epsilon \frac{1}{2} \frac{1+\lambda^2}{1-\lambda^2} \left\{ \gamma \cos 2\phi - u^{-1} \cos 2(\theta - \phi) \right\} + \epsilon\alpha \frac{\gamma}{2} + O(\epsilon^3).$$

(52) expresses the following sequence of interactions. On the $O(1)$ time scale, the elliptical vortices rotate at a rate $\lambda/(1+\lambda)^2$. On a longer time scale, $O(\epsilon^{-1})$, the aspect ratio and rotation rate of the vortices slowly vary. The vortices move in the background shear flow and under the influence of their mutual interaction on this same time scale. On an even longer

time scale, $O(\epsilon^{-2})$, the finite size of the vortices induce small perturbations to the rate at which the vector separating their centroids changes.

IV. ASYMPTOTIC ANALYSIS

In this section, we investigate the system (52) by means of an asymptotic analysis in the small parameter ϵ. We use the Melnikov approach[22,30–31] and appeal to analogies between this system and a rapidly forced pendulum.

We begin by reminding the reader of how the Melnikov integral measures the distance between the stable and unstable manifolds formed by the splitting of a homoclinic or heteroclinic orbit. We shall consider its most commonly encountered variant, that for a periodically perturbed one degree-of-freedom Hamiltonian system:

$$\dot{q} = \frac{\partial H}{\partial p}(q,p), \qquad \dot{p} = -\frac{\partial H}{\partial q}(q,p), \tag{53}$$

where

$$H = H_0(q,p) + \epsilon H_1(q,p,t), \tag{54}$$

and H_1 is an explicit periodic function of the time variable, t. Let the explicit period of H_1 be τ and let this be $O(1)$. Setting $z(t) = (q(t), p(t))$, we consider the case in which the unperturbed system has two hyperbolic fixed points which are joined by a heteroclinic orbit $z(t) = z_0(t)$. (The homoclinic case is analogous.) If one defines a function M of $t_0 \in (-\infty, \infty)$ by

$$M(t_0) = \epsilon \int_{-\infty}^{\infty} \{H_0(z_0(t)),\, H_1(z_0(t), t + t_0)\}\, dt, \tag{55}$$

then the signed separation between the stable and unstable manifolds along the normal to the unperturbed separatrix is given by

$$d(t_0) = \frac{M(t_0)}{\mid H_0(z_0(t_0)) \mid} + O(\epsilon^2). \tag{56}$$

The existence of one zero of $M(t_0)$ implies the existence of infinitely many zeroes since $M(t_0)$ is periodic with period τ. (H_1 is periodic in its last argument.) And if $\partial M(t_0)/\partial t_0 \neq 0$ at these points, there are infinitely many transverse manifold crossings and thus chaotic motion in the vicinity of the separatrix. It is M that we refer to as the Melnikov function or Melnikov integral.

The system (52) is not of the form required for the standard Hamiltonian Melnikov analysis. To begin with, the variables are not canonical; but this is only a question of coordinates. Next, the basic state that we would like to perturb around, that of a pair of point vortices in shear, is a one degree-of-freedom system, while the full system (52) has two degrees of freedom. Most importantly, there are two distinct time scales: the natural time scale for the centroidal motion is $O(\epsilon^{-1})$; the time scale for the rotation of the vortices is $O(1)$ and terms containing ϕ appear in the other three equations. The slow centroidal motion is coupled with fast variations in the vortices' orientation and shape, complicating the analysis.

These difficulties can be resolved within a perturbative, multiple time-scale setting. An explicit time-periodic perturbation to the Hamiltonian is not given, but in some parameter ranges, the second degree of freedom, (λ, ϕ), behaves like an oscillator and the variable ϕ increases monotonically with time. One can consider the first degree of freedom, (u, θ), to be "perturbed" by this second degree of freedom. By transforming the autonomous two degree-of-freedom system (52) into a nonautonomous one degree-of-freedom system where the slow centroid motion is perturbed by the fast oscillatory terms of the $\dot{u}$, $\dot{\theta}$ and $\dot{\lambda}$ equations, a multiple time-scale analysis can then be performed.

There is a growing body of research on Hamiltonian systems with rapidly oscillating perturbations. The implications of this research for our system are briefly examined in the next section.

A. The rapidly, but weakly, forced pendulum

Since there are two time scales in the restricted vortex system of (52), and the fast oscillatory terms occur at higher order in ϵ, we expect its behavior to be analogous to that of a nonlinear pendulum forced by a weak but rapid oscillation, viz.

$$\frac{d^2x}{dt^2} + \sin x = \delta \sin\left(\frac{t}{\epsilon}\right), \tag{57}$$

where $\delta\epsilon^{-n} \to 0$ for an appropriate positive power n.[26,32–33] This is of the form shown in (53) with

$$q = x, \quad p = \dot{x}, \qquad H_0 = \frac{1}{2}p^2 - \cos q, \quad H_1 = -q\delta \sin(t/\epsilon).$$

When $\delta = 0$, the unperturbed system is a one degree-of-freedom Hamiltonian system with a hyperbolic fixed point at $(x = 0, \dot{x} = 0)$ and a homoclinic trajectory emanating from it (identifying $x = 2\pi$ with $x = 0$). As is standard with nonautonomous systems, one can define a Poincaré section by strobing the system at the period of the forcing, $2\pi\epsilon$. For sufficiently weak forcing, the associated Poincaré map has a hyperbolic fixed point that lies close to the unperturbed one. In certain cases, it can be shown that the stable and unstable manifolds persist, lie close to the unperturbed homoclinic orbit, and intersect transversally.[33]

In the periodically forced Hamiltonian system described at the beginning of Sec. IV, the splitting distance between the stable and unstable manifolds is $O(\epsilon)$ and is given by the Melnikov integral (56). For the rapidly forced system (57), the Melnikov integral is exponentially small; but the meaning of this is uncertain because formally, the Melnikov distance is only accurate to $O(\epsilon^2)$. It is, however, now thought that under properly specified conditions, the Melnikov analysis generally does provide a good estimate of the splitting distance.[25] Kummer *et al.* (1991)[33] were able to establish that the leading order term in the splitting distance is indeed given by a Melnikov analysis when $n = 5$. It is conjectured that a similar result holds when $n = 1$—which is in essence the case for the system (52). The

proof of this, and of the exponentially small nature of the splitting distance, exploits the explicit closed-form representation of the unperturbed system's homoclinic trajectory. (This allows the contours of integration of certain integrals to be moved in the complex plane.) In the problem at hand, we cannot provide such proofs, largely because we have an implicit representation only. Nevertheless, we argue that the structural similarity of the rapidly forced pendulum to the restricted vortex system suggests that in the latter, the manifolds should cross transversally and the separatrix splitting should be exponentially small. We provide support for this by performing a Melnikov analysis and examining the leading order contribution to the splitting distance. This does not constitute a proof because in this asymptotic analysis, an infinite series of integrals contributes to the splitting distance and they may not all be exponentially small.

We will later turn to numerical simulations to see if they are are in accord with this picture.

B. Calculating a Melnikov function

We now present a Melnikov analysis which freely exploits a number of assumptions. To begin with, we exploit the autonomous nature of the system and restrict our attention to situations in which the vortex orientation, ϕ, increases monotonically with time. Provided there are trajectories for which λ can be bounded away from 1, the form of (52) suggests that this is reasonable for small ϵ. This allows us to replace the independent variable t with ϕ:

$$\frac{du}{d\phi} = Q\left[\epsilon\gamma u \sin 2\theta - \epsilon^2 u^{-1}\frac{1-\lambda^2}{\lambda}\sin 2(\theta-\phi)\right] \tag{58}$$

$$\frac{d\theta}{d\phi} = Q\left[\epsilon\left\{\frac{\gamma}{2}(\alpha+\cos 2\theta)+u^{-1}\right\}+\epsilon^2\frac{1}{2}u^{-2}\frac{1-\lambda^2}{\lambda}\cos 2(\theta-\phi)\right]$$

$$\frac{d\lambda}{d\phi} = -Q\left[\epsilon\lambda\left\{\gamma\sin 2\phi + u^{-1}\sin 2(\theta-\phi)\right\}\right]$$

where

$$Q = \left\{ \frac{\lambda}{(1+\lambda)^2} + \epsilon \frac{1}{2} \frac{1+\lambda^2}{1-\lambda^2} \left\{ \gamma \cos 2\phi - u^{-1} \cos 2(\theta - \phi) \right\} + \epsilon\alpha \frac{\gamma}{2} \right\}^{-1}. \tag{59}$$

Next, the conservation of the Hamiltonian is invoked to express $\lambda = \lambda(u, \theta, \phi; h)$ and eliminate λ from the first two equations (58). The resulting system may be written in the form

$$\begin{aligned} \frac{du}{d\phi} &= F_1(u, \theta, \lambda(u, \theta, \phi)) + f_1(u, \theta, \lambda(u, \theta, \phi), \phi) \\ \frac{d\theta}{d\phi} &= F_2(u, \theta, \lambda(u, \theta, \phi)) + f_2(u, \theta, \lambda(u, \theta, \phi), \phi), \end{aligned} \tag{60}$$

where

$$F_1 = \epsilon\Omega\gamma u \sin 2\theta, \qquad F_2 = \epsilon\Omega \left\{ \frac{\gamma}{2} (\alpha + \cos 2\theta) + u^{-1} \right\}, \qquad \Omega = \Omega(\lambda) = \left\{ \frac{\lambda}{(1+\lambda)^2} + \epsilon\alpha \frac{\gamma}{2} \right\}^{-1},$$

$$f_1 = Q \left[\epsilon\gamma u \sin 2\theta - \epsilon^2 u^{-1} \frac{1-\lambda^2}{\lambda} \sin 2(\theta - \phi) \right] - \epsilon\Omega\gamma u \sin 2\theta, \tag{61}$$

$$f_2 = Q \left[\epsilon \left\{ \frac{\gamma}{2} (\alpha + \cos 2\theta) + u^{-1} \right\} + \epsilon^2 \frac{1}{2} u^{-2} \frac{1-\lambda^2}{\lambda} \cos 2(\theta - \phi) \right] - \epsilon\Omega \left\{ \frac{\gamma}{2} (\alpha + \cos 2\theta) + u^{-1} \right\}.$$

We would like to obtain a one degree-of-freedom system whose basic state is given by the equations of motion for a point vortex pair in shear. The functions F_1 and F_2 have the correct form, but they do not constitute a proper basic state as they are a coupled to the perturbed motion through $\Omega(\lambda)$. We therefore expand λ in a perturbation series

$$\lambda = \lambda_0 + \epsilon\lambda_1(\phi) + \ldots, \tag{62}$$

where λ_0 is a constant and can be treated as a parameter. (This is permissible for trajectories with λ bounded away from 0 and 1.) The function $\Omega(\lambda)$ can then be expanded in ϵ and its leading order component,

$$\Omega_0 = \left\{ \frac{\lambda_0}{(1+\lambda_0)^2} + \epsilon\alpha \frac{\gamma}{2} \right\}^{-1}, \tag{63}$$

used to define an appropriate basic state.

We now write

$$\frac{du}{d\phi} = G_1(u,\theta;\Omega_0) + g_1(u,\theta,\phi) \tag{64}$$

$$\frac{d\theta}{d\phi} = G_2(u,\theta;\Omega_0) + g_2(u,\theta,\phi),$$

with

$$G_1 = \tilde{G}_1 + \tilde{g}_1 = \epsilon\Omega_0\gamma u \sin 2\theta + \tilde{g}_1, \tag{65}$$

$$G_2 = \tilde{G}_2 + \tilde{g}_2 = \epsilon\Omega_0 \left\{ \frac{\gamma}{2}(\alpha + \cos 2\theta) + u^{-1} \right\} + \tilde{g}_2.$$

By construction, G_1 and G_2—and thus the tilde quantities—have no explicit ϕ dependence while g_1 and g_2 have an explicit π-periodic dependence on ϕ. The functions $\tilde{g}_1$ and g_1 may be obtained from

$$\mathcal{G}_1 = Q\left[\epsilon\gamma u \sin 2\theta - \epsilon^2 u^{-1} \frac{1-\lambda^2}{\lambda} \sin 2(\theta - \phi)\right] - \epsilon\Omega_0\gamma u \sin 2\theta;$$

and g_2 and $\tilde{g}_2$ may be obtained from

$$\mathcal{G}_2 = Q\left[\epsilon\left\{\frac{\gamma}{2}(\alpha + \cos 2\theta) + u^{-1}\right\} + \epsilon^2 \frac{1}{2} u^{-2} \frac{1-\lambda^2}{\lambda} \cos 2(\theta - \phi)\right]$$

$$-\epsilon\Omega_0 \left\{\frac{\gamma}{2}(\alpha + \cos 2\theta) + u^{-1}\right\}.$$

(Note that while F_1, F_2, G_1 and G_2 are $O(\epsilon)$, f_1, f_2, g_1 and g_2 are $O(\epsilon^2)$.) The basic state is given by

$$\frac{du}{d\phi} = \tilde{G}_1 = \epsilon\Omega_0\gamma u \sin 2\theta \tag{66}$$

$$\frac{d\theta}{d\phi} = \tilde{G}_2 = \epsilon\Omega_0 \left\{\frac{\gamma}{2}(\alpha + \cos 2\theta) + u^{-1}\right\}.$$

Identifying $\Phi = \epsilon\phi$ as a slow time, these are indeed the equations of motion for a pair of point vortices in shear. Ω_0 can be interpreted as a parameter set by the initial conditions.

Without loss of generality, we assume that $\gamma > 0$ ($\gamma < 0$ just rotates the phase space through 90 degrees), and that $\alpha < 1$ (a sufficient condition for the existence of hyperbolic fixed points; see the Appendix).

We can now proceed along the lines of the standard Melnikov analysis. By analogy with other 1.5 degree-of-freedom systems, a Poincaré section is defined on the plane $\phi = \phi_p \pmod{\pi}$, $\phi_p \in (-\infty, \infty)$ being an arbitrary constant. (Formally, we transform to an autonomous third-order system and plot intersections of its trajectories with $\phi = \phi_p \pmod{\pi}$.) In the unperturbed limit, the associated Poincaré map has hyperbolic fixed points at $(u, \theta) = (2/[\gamma(1-\alpha)], \pm\pi/2)$ which are joined by a pair of invariant heteroclinic manifolds. The smoothness of the system means that for any closed, compact range of λ that does not include $\lambda = 0$ or 1, the hyperbolic points persist for sufficiently small ϵ. It is therefore expected that a perturbation will split the heteroclinic manifolds into distinct stable and unstable manifolds.

Let $q_0(\phi) = (u_0(\epsilon\phi), \theta_0(\epsilon\phi))$ be a heteroclinic trajectory of the unperturbed system. Since the unperturbed system is autonomous, $q_0(\phi)$ passes through all the points on the unperturbed heteroclinic manifold as ϕ increases from $-\infty$ to ∞ (i.e. from fixed point to fixed point). In the usual way, a set of coordinates on the heteroclinic manifold is then defined by a choice of the point $q_0(0)$. Trajectories on the perturbed stable and unstable manifolds can be obtained by expanding around this heteroclinic trajectory:

$$q^j(\phi; \phi_p, \epsilon) = q_0(\phi - \phi_p) + q_1^j(\phi; \phi_p), \tag{67}$$

where $j = s$ or u. The deviation q_1^u is asymptotically small (in ϵ) compared to q_0 as $\phi \to -\infty$; q_1^s is asymptotically small compared to q_0 as $\phi \to +\infty$. Actually, $u_1 \sim O(\epsilon^2)$ and $\theta_1 \sim O(\epsilon^2)$. Note that we have exploited the autonomous nature of the unperturbed system once more in shifting the time origin $\phi = 0$: for each particular choice of ϕ_p, the heteroclinic trajectory is now given by $q_0(\phi - \phi_p)$.

We seek an estimate of the distance between these manifolds at a point $q_0(0)$ and in a direction normal to the unperturbed heteroclinic orbit. Letting $G = (G_1(q), G_2(q))$, (64) can be rewritten as

$$\frac{dq}{d\phi} = G(q) + g(q, \phi), \tag{68}$$

and the normal to the unperturbed invariant manifold is

$$\tfrac{1}{2}\, t\boldsymbol{n} = (-G_2(q_0), G_1(q_0))/(G_1(q_0)^2 + G_2(q_0)^2)^{1/2} = \boldsymbol{n}/(G_1(q_0)^2 + G_2(q_0)^2)^{1/2}. \tag{69}$$

The transverse splitting distance at $q_0(\phi = 0)$ is then given by

$$d(\phi_p) = M(\phi_p)/[G_1^2(q_0(0)) + G_2^2(q_0(0))]^{1/2}, \tag{70}$$

where

$$M(\phi_p) = \Delta^s(\phi_p; \phi_p) - \Delta^u(\phi_p; \phi_p) \tag{71}$$

and

$$\Delta^j(\phi; \phi_p) = \boldsymbol{n} \cdot q_1^j(\phi; \phi_p) = G_1(q_0(\phi - \phi_p))\theta_1^j(\phi; \phi_p) - G_2(q_0(\phi - \phi_p))u_1^j(\phi; \phi_p). \tag{72}$$

In order to calculate $M(\phi_p)$, and thus the splitting distance, the system (64) must be expanded. As $G(q_0) = F(q_0, \lambda_0)$ and likewise for g and f, the quantities Δ^j and q_1^j may be expressed in terms of f and F, simplifying the calculations. Expanding:

$$\frac{d\Delta^j}{d\phi} = \left(\frac{dF_1}{dq}\right)_{q_0,\lambda_0} \cdot \frac{dq_0}{d\phi}\theta_1^j - \left(\frac{dF_2}{dq}\right)_{q_0,\lambda_0} \cdot \frac{dq_0}{d\phi}u_1^j + (F_1)_{q_0,\lambda_0}\frac{d\theta_1^j}{d\phi} - (F_2)_{q_0,\lambda_0}\frac{du_1^j}{d\phi} \tag{73}$$

$$= \left(F_1\frac{\partial F1}{\partial u} + F_2\frac{\partial F_1}{\partial \theta}\right)_{q_0,\lambda_0}\theta_1^j - \left(F_1\frac{\partial F2}{\partial u} + F_2\frac{\partial F_2}{\partial \theta}\right)_{q_0,\lambda_0}u_1^j$$

$$+(F_1)_{q_0,\lambda_0}\frac{d\theta_1^j}{d\phi} - (F_2)_{q_0,\lambda_0}\frac{du_1^j}{d\phi};$$

and

$$\frac{dq_1^j}{d\phi} = F\left(q_0(\phi-\phi_p)+q_1^j(\phi,\phi_p),\ \lambda_0+\lambda_1^j\right) - F\left(q_0(\phi-\phi_p),\lambda_0\right) \tag{74}$$

$$+f\left(q_0(\phi-\phi_p)+q_1^j(\phi,\phi_p),\lambda_0+\lambda_1^j,\phi\right)$$

$$\sim \left(\frac{\partial F}{\partial u}u_1^j+\frac{\partial F}{\partial\theta}\theta_1^j+\frac{\partial F}{\partial\lambda}\lambda_1^j\right)+\left(\frac{1}{2}\frac{\partial^2 F}{\partial\lambda^2}\lambda_1^j\lambda_1^j+...\right)+...$$

$$+f\left(q_0(\phi-\phi_p),\lambda_0,\phi\right)+q_1^j\cdot\left(\frac{df}{dq}\right)_{q_0,\lambda_0}+\lambda_1^j\left(\frac{df}{dq}\right)_{q_0,\lambda_0}+....\ .$$

Since F_1 and F_2 have the form

$$F_1 = p(\lambda)\frac{\partial}{\partial\theta}P(u,\theta), \qquad F_2 = -p(\lambda)\frac{\partial}{\partial u}P(u,\theta),$$

many terms on the right-hand side of (73) cancel and

$$\frac{d\Delta^j}{d\phi} = F_1(q_0(\phi-\phi_p),\lambda_0)f_2(q_0(\phi-\phi_p),\lambda_0,\phi)-F_2(q_0(\phi-\phi_p),\lambda_0)f_1(q_0(\phi-\phi_p),\lambda_0,\phi)$$

$$+\lambda_1\left(F_1\frac{\partial f_2}{\partial\lambda}-F_2\frac{\partial f_1}{\partial\lambda}\right)+u_1\left(F_1\frac{\partial f_2}{\partial u}-F_2\frac{\partial f_1}{\partial u}\right)$$

$$+\theta_1\left(F_1\frac{\partial f_2}{\partial\theta}-F_2\frac{\partial f_1}{\partial\theta}\right)+...,$$

which is formally $O(\epsilon^3)$ at leading order. Let us write this as

$$\frac{d\Delta^j}{d\phi} = \epsilon^3 T_1+\epsilon^4 T_2+\epsilon^5 T_3+...\ . \tag{75}$$

The forms of the f's are rather complicated, however. We can simplify the manipulation of them by expanding in ϵ, e.g.

$$f_2(q_0,\lambda_0,\phi) = f_{20}(q_0,\lambda_0,\phi)+\epsilon f_{21}(q_0,\lambda_0,\phi)+...\ .$$

This induces corresponding expansions in the T's:

$$T_j = T_{j0}+\epsilon T_{j1}+... \tag{76}$$

and (75) becomes

$$\frac{d\Delta^j}{d\phi} = \epsilon^3 T_{10} + \epsilon^4 (T_{20} + T_{11}) + \dots \,.$$

Integrating the preceding equation over ϕ yields $M(\phi_p)$:

$$M(\phi_p) = \epsilon^3 M_{10}(\phi_p) + \epsilon^4 \left(M_{20}(\phi_p) + M_{11}(\phi_p)\right) + \dots \,. \tag{77}$$

The leading order contribution is fairly easy to calculate. With $\Omega_0 = \Omega(\lambda_0)$, we find that

$$T_{10} = \frac{1}{2} \frac{1-\lambda_0^2}{\lambda_0} \Omega_0^2 u_0^{-1} \left\{ \gamma \sin(4\theta_0 - 2\phi) + (\gamma\alpha + 2u_0^{-1}) \sin 2(\theta_0 - \phi) \right\}. \tag{78}$$

Therefore,

$$\begin{aligned} M_{10}(\phi_p) &= \int_{-\infty}^{\infty} T_{10} d\phi \qquad (79) \\ &= -\frac{1}{2} \frac{1-\lambda_0^2}{\lambda_0} \Omega_0^2 \sin 2\phi_p \int_{-\infty}^{\infty} u_0^{-1} \left\{ \gamma \cos[4\theta_0(\epsilon\phi) - 2\phi] \right. \\ &\qquad \left. + (\gamma\alpha + 2u_0^{-1}(\epsilon\phi)) \cos[2\theta_0(\epsilon\phi) - 2\phi] \right\} d\phi. \end{aligned}$$

We have chosen the origin of the ϕ coordinate so that $\theta_0(0) = 0$, i.e. the midpoint of the heteroclinic trajectory.

From the leading $\sin 2\phi_p$ factor, we see that M_{10} crosses zero infinitely many times. By a generalized Riemann-Lebesgue lemma,[34] the integral is $\ll O(\epsilon^n)$ for any n: it is exponentially small in ϵ. A necessary (but not sufficient) condition for this to be the dominant part of $M(\phi_p)$ is that the higher-order corrections, M_{11}, M_{20}, etc., must also be at most exponentially small. While this is at least possible for those T_{mn} that are rapidly oscillating functions of ϕ, if there are any parts of T_{mn} that have no fast time dependence, then we must consider their contribution to M more carefully. Below we will find the leading order term with only slow ϕ dependence and show that it makes zero contribution to M.

We need to compute $T_{20}+T_{11}$. This requires a knowledge of the first asymptotic correction to the path of the perturbed stable and unstable manifolds. It can be shown that the first

correction to λ is

$$\lambda_1 = \frac{1}{2}\lambda_0\Omega_0\left\{\gamma\cos 2\phi - u_0^{-1}\cos 2(\theta_0-\phi)\right\}.$$

Then

$$T_{20} = -\left\{\frac{\Omega_0^3}{2\lambda_0}\frac{(1-\lambda_0)^2}{(1+\lambda_0)^2} + \frac{1}{2}\Omega_0^2\frac{1+\lambda_0^2}{\lambda_0^2}\right\}$$
$$\times u_0^{-1}\lambda_1\left\{\gamma\sin(4\theta_0-2\phi) + (\gamma\alpha+2u_0^{-1})\sin(2\theta_0-2\phi)\right\}$$

$$T_{11} = -\frac{1}{2}\Omega_0^2\frac{1+\lambda_0^2}{\lambda_0^2}u_0^{-1}\lambda_1\left\{\gamma\sin(4\theta_0-2\phi) + (\gamma\alpha+2u_0^{-1})\sin(2\theta_0-2\phi)\right\}.$$

Upon substituting for λ_1, we find that the sum $T_{20}+T_{11}$ consists of two parts: a rapidly oscillating component, T_{2f}, that like T_{10}, yields an exponentially small contribution upon integration; and another component, T_{2s}, that does not oscillate rapidly. In principle, this should result in a contribution to the Melnikov integral which is not exponentially small and so would dominate M_{10}. However, if we calculate T_{2s} explicitly, we find that

$$T_{2s} = -\left\{\frac{\Omega_0^4(1-\lambda_0)^2}{(1+\lambda_0)^2} + 2\Omega_0^3\frac{1+\lambda_0^2}{\lambda_0}\right\}\frac{1}{8}\gamma u_0^{-1}\left\{\gamma\sin(4\theta_0) + (\gamma\alpha+u_0^{-1})\sin(2\theta_0)\right\}. \qquad (80)$$

This is symmetric about $\phi=\phi_p$, so the integral $\int_{-\infty}^{\infty}d\phi$ is identically zero, and the slow component of $M_{20}+M_{11}$ thus vanishes. As for slow perturbations to the positions of the stable and unstable manifolds, there is a part of u_1 and θ_1 which does not oscillate rapidly, but it affects both manifolds in the same way and so does not contribute to the splitting distance at this order. We note that the correction $\epsilon^4(M_{20}+M_{11})$ formally occurs at the same order as would the corrections associated with deviations of the shape of the vortices from ellipticity (i.e. $O(\epsilon^3)$).

V. NUMERICAL RESULTS

The Melnikov analysis suggests that a chaotic band may form around the unperturbed separatrix, though the (exponentially small) scaling is rather tentative. Here we use numerical simulations to both confirm this and provide a picture of the global dynamics. For

simplicity, only the ϵ dependence will be considered at length. The equations of motion (47) are used for the integrations; the singularity at $\lambda = 1$ has not caused any difficulty.

A. Poincaré sections

We construct Poincaré sections for the two degree-of-freedom Hamiltonian system (52) by first choosing a value H_0 for the Hamiltonian. A Poincaré section is then built-up by computing trajectories from a set of initial conditions which satisfy $H(\lambda; u, \theta, \phi = 0) = H_0$. Whenever $\phi(t) = 0 \pmod{\pi}$ in a specified sense (increasing for $\Gamma_i > 0$),[35] a point appears on the three-dimensional Poincaré section spanned by u, θ and λ; it is then projected onto the (u, θ) plane. The results are shown in (x, y) coordinates by applying the transformation $(x, y) = u^{1/2}(\cos\theta, \sin\theta)$.

For each Poincaré section, H_0 is fixed by evaluating H for a given ($x = x_0$, $y = y_0$, $\lambda = \lambda_0$; $\phi = 0$) using (48). A set of initial conditions satisfying $H = H_0$ is obtained by specifying x, y, ϕ and solving the nonlinear equation

$$H(\lambda; u, \theta, \phi = 0) = H_0$$

for λ. (A bracketing-bisection scheme is used.) For $\epsilon = 0.01$ to $\epsilon = 0.03$, we have observed a maximum of 3 roots, the number depending on the value of H_0 and the limits, $\lambda_{\min}, \lambda_{\max}$, between which roots are found. The limits span the range of λ over which the model is expected to be (initially) valid. In most of the cases discussed below, H_0 corresponds to a point on the unperturbed separatrix. With a linear shear flow $(e, \omega) = (1/\pi, -1/\pi)$ and $\Gamma = 1$, the fixed points are located at $(x_0, y_0) = (0, \pm 1/(\pi e)) = (0, \pm 1)$; H_0 is determined using $(x_0, y_0, \lambda_0 = (0, 1, 1.5)$. We thus take $D = 1$ in our definition of ϵ.

In Fig. 2a, the Hamiltonian surface for $\epsilon = 0.01$ without shear (i.e. $A = \pi/100$) is shown: it is a closed surface that does not extend beyond the cylinder $u := x^2 + y^2 = 1$. The Hamiltonian surface looks very different once shear is added. In Fig. 2b, a Hamiltonian

surface for $\epsilon = 0.01$ with shear is shown: the surface now fans-out beyond the unperturbed separatrix. As it is smooth, all points on the surface are, in principle, accessible to one another. Any point on the Hamiltonian surface, even those beyond the separatrix, should be able to reach the cusp at the origin. In what follows, $u \rightarrow 0$ and vortex merger are used interchangeably.

Poincaré sections are shown in Fig. 3. For the MZS model, closed orbits encircle the origin, but at a distance (Fig. 3a). There is a large gap in the interior where there are no (closed) orbits at all; initial conditions that are too close to the origin merge before appearing on a Poincaré section. Moving away from the origin, one sees that closed orbits do not, in agreement with Fig. 2a, extend beyond $u^2 = 1$. For $\epsilon = 0.01$, there are, as with the point vortex pair in shear, closed orbits inside the separatrix, and unbounded orbits outside (Fig. 3b). There is also a gap in the interior. When ϵ is increased, bounded and unbounded orbits remain, but there are far fewer of them: the fraction of merging initial conditions increases rapidly with ϵ. For $\epsilon = 0.03$, every point inside the unperturbed separatrix merges (Fig. 3c).

In the absence of shear, the innermost orbit of the Poincaré section divides initial conditions which merge from those that do not: it defines a critical merger criterion. This criterion is *not*, however, the same as the classical criterion for identical circular vortices, i.e. that the critical separation, $r_c = 3.3\, r_v$ where r_v is the vortex radius (see MZS). The Poincaré section is defined at constant H, not constant λ. In general, it is expected that the critical merger threshold defined on a constant Hamiltonian surface, $r_{c,H}$, will be greater than r_c, with $\min_H(r_{c,H}) = r_c$. Even for a Poincaré section associated with near-circular vortices at the separatrix, $r_{c,H}$ is quite different from r_c because the vortices are strongly elongated away from the separatrix. For example, $r_{c,H} \approx 0.61 = 0.61 r_v$ and $\lambda(r_{c,H}) \approx 10$ when $\lambda_0 = 1.001$ and $\epsilon = 0.01$. In Fig. 4, we show a merging trajectory corresponding to Fig. 3a—note that

r is initially less than $r_{c,H}$.

An innermost orbit can also be distinguished in Fig. 3b (i.e. $\epsilon = 0.01$ with shear), but it cannot be associated with a critical merger threshold in the same way as the MZS model. Because of the presence of the background shear, it is now possible for points outside the separatrix to merge; the regions of the Poincaré section inside and outside the unperturbed separatrix are no longer perfectly separated. Most of the exterior trajectories are analogous to the unbounded orbits for a point vortex pair in shear—physically, the vortices approach one another, reach a minimum separation, and are carried away by the shear—but the combined effect of vortex-vortex and vortex-shear interactions now makes merger possible for a small fraction of them (Fig. 5). In cases where ϵ is small, the innermost orbit defines a critical radius that separates *most* of the merging orbits from *most* of the non-merging orbits (e.g. Fig. 3b), the exchange between the interior and the exterior being rather limited.

The kind of merger represented by Fig. 5 is very different from that in Figs. 3a and 4. Whereas vortex-vortex interactions dominated the previous mode of merger vortex-shear interactions are crucial to this one: vortex-shear interactions stretch the vortices out and bring them together; vortex-vortex interactions then initiate the actual merger. For a typical merging trajectory initially outside the separatrix (Fig. 6), λ is initially greater than $\lambda_{\min}$, the lower limit for the bracketing-bisection scheme, but considerably less than $\lambda_{\min}$ by the time the trajectory crosses the separatrix. (These trajectories do not appear on the Poincaré section because they merge before ϕ goes through π.) During the course of merger, the approximation that the vortices are small and well-separated breaks down; but this does not mean that this second mode of merger is a numerical artifact. Such a mechanism has been observed in contour dynamics simulations of circular vortices in shear.[36] In any case, it is inevitable that the model break down during merger—this also occurs for the other mode of merger, the vortex-vortex one.

Melander *et al.* (1988)[11] derived a merger criterion for the MZS model which agrees

fairly well with contour dynamics simulations. When ambient shear is present, there does not appear to be an analytical expression, based on the initial configuration of the vortex pair, which concisely summarizes when they will and will not merge. A merger criterion for initial conditions inside the separatrix could be determined by estimating the position of the innermost orbit on the Poincaré section; but the situation is much more complicated for initial conditions outside the separatrix. Outside the separatrix, vortex merger is the result of a very complex interplay between vortex-vortex and vortex-shear interactions. Many initial conditions yield trajectories which approach the separatrix, but most of these do not merge. A small displacement in (u, θ) can make the difference between merger and separation by the shear. Another complicating factor is that for larger values of ϵ, there is vortex-vortex merger for points lying just outside the separatrix and initial $\lambda \gg 1$.

B. Separatrix splitting and chaos

Because the Melnikov result is an asymptotic one and because the Melnikov function is exponentially small, numerical verification of the formation of a heteroclinic tangle is needed.

Verification of the exponentially small nature of the numerator in the expression for the separatrix splitting distance is difficult since the position of the folds is a function of ϵ (though the slow time $\Phi = \epsilon\phi$), and the folds will narrow and squeeze together as ϵ is reduced. Moreover, the denominator in (70) also becomes exponentially small as one approaches the hyperbolic points, where the splitting is greatest. The important result is not the precise scaling, but the existence of the heteroclinic tangle and the fact that the splitting is generally small. It could be possible for the stable and unstable manifolds to split apart, but not intersect transversally.

Figure 7a shows a blow-up of the $\epsilon = 0.01$ Poincaré section around the separatrix, while Fig. 7b shows a typical trajectory in this region. Though we anticipate that a heteroclinic tangle is present, its width is too narrow to be resolved by these pictures; one must look very

closely around the separatrix for any evidence of the separatrix splitting. For larger values of ϵ, the separatrix splitting is clearly evident: there are distinct fold-like structures for $\epsilon = 0.03$ (Fig. 3c). This is very reminiscent of a heteroclinic tangle. Most trajectories, however, do not follow these structures indefinitely: they usually merge after a short while. This explains the fuzziness of Fig. 3c. Nevertheless, as with other systems containing a heteroclinic tangle, there is an associated chaotic invariant set.

The separatrix splitting would appear to be relevant to vortex merger as there are only a limited number of initial conditions outside the separatrix that lead to merger, but the relationship is not so simple. The separatrix splitting applies to that portion of the Hamiltonian surface where $\lambda = O(1)$, and not to the small λ states associated with exterior vortex merger. Indeed this behavior could not be predicted from the Hamiltonian surface of Fig. 2b because that figure does not cover a wide enough range of λ. (Recall also that the Melnikov analysis only applies to small perturbations about a basic state.) The separatrix splitting does have an effect on vortex merger insofar as orbits with $\lambda \approx O(1)$ do not cross the separatrix, but this is an indirect effect at best.

The neighborhood around the separatrix is not the only region in which we find chaotic zones. Figure 8a is a blow-up of the Poincaré section between $r = 0.50$ and $r = 0.40$; Fig. 8b is a typical trajectory in this region. The trajectories hop around chaotically until they fall into the origin (i.e. the vortices merge). This inner chaotic region provides an example of chaos associated with a higher-order resonance,[37] 9:1 to be precise, between the natural frequency of periodic contours in the unperturbed system and that of the perturbation. The order of the resonance decreases as one approaches the origin, as would be expected.

As far as we can determine, trajectories spend only a finite amount of time in the chaotic regions. This is evidently a system in which chaotic transients play an important role. Immediately inside the unperturbed separatrix, we have seen that there are (weakly) chaotic

trajectories (e.g. Figs. 3c and 7). For trajectories originating outside the separatrix, the chaotic transients could give rise to chaotic scattering. Chaotic scattering is usually manifested in rapid fluctuations of a scattering angle θ_s (defined in terms of the initial and final separation vectors) with respect to an impact parameter (some function of the initial separation angle or distance).[38–39] The variations occur on all scales and are strongly correlated with singularities or peaks in the residence time. The latter, which are just interaction times, form a fractal set.

We use the angle of incidence θ_i as an impact parameter. It is varied while the initial radial separation r_i is fixed. The scattering angle θ_s is computed when the final separation $r_\mathrm{f} = r_\mathrm{i}$, after the closest approach of the vortices. It is convenient to define θ_s in terms of θ_i and the final centroidal angle, θ_f: $\theta_s = \theta_i + \theta_f - \pi$ so that $\theta_s = 0$ corresponds to reflection about the line $y = 0$, and $\theta_s = \pi$ to reflection about $x = 0$. The residence time is determined by the condition $r < r_\mathrm{i}$.

In Fig. 9a, θ_s is plotted against $\theta_i \in (\pi/2, \pi)$ for $\epsilon = 0.01$ and $r_\mathrm{i} = 1.1$. Instead of assuming a continuous range of values, as is normally the case in chaotic scattering, θ_s assumes only the values $\theta_s = 0$ and $\theta_s = \pi$ for this set of parameters. Because of the background shear, there are only two possible outcomes to a scattering event: a trajectory can be carried off towards increasing y ($\theta_s = 0$), or towards decreasing y ($\theta_s = \pi$). (These trajectories correspond to the two types of unbounded orbits present in the Poincaré section of Fig. 3b.) Moreover, the vortices scatter only once before they are separated by the shear. This can be seen in Fig. 9b, where the residence time is plotted against θ_i. The residence time varies smoothly with θ_i and there is no evidence of fractal structure or of multiple scattering events.

Nevertheless, the scattering is chaotic. If one looks very closely, there are, as would be expected, weak oscillations in θ_s (Fig. 9c). Despite the absence of multiple interactions and strong oscillations in θ_s, the vortices do scatter chaotically as θ_s is not a perfectly smooth function of θ_i. This is related to the existence of a nonattracting—but spatially extended—

chaotic invariant set. The scattering angle θ_s exhibits sensitive dependence on the incident angle θ_i. This kind of scattering is quite different from that described in previous studies of chaotic scattering in vortex dynamics.[40–41] In these studies, the scattering can be represented symbolically in terms of the exchange of different or like signed vortices.

VI. DISCUSSION

We began this paper by deriving the equations of motion for N elliptical vortices in a background shear flow. This model is identical to that of Melander *et al.* (1986)[2] except for the background shear (which combines rotation and shear). With this in mind, the majority of this paper represents an attempt to understand what happens when vortex-shear interactions are added, specifically the implications for vortex merger. The numerical computations presented in the last part of this paper vividly illustrate the effect of vortex-shear interactions and the complex interplay that exists between vortex-shear and vortex-vortex interactions. Besides vortex merger, these interactions are manifested in chaotic motion and a (weak) form of chaotic scattering. The Melnikov analysis of Sec. IV was motivated by the expectation that the magnitude of the separatrix splitting would profoundly influence the merger of initially well-separated vortices. The separatrix for a point vortex pair in shear divides the interior from the exterior; with a perturbation, the addition of internal degrees of freedom, the separatrix splits into stable and unstable manifolds which intersect transversely, giving rise to a heteroclinic tangle and transport across the separatrix. In analogy with results for rapidly forced oscillators,[32–33] the Melnikov function is exponentially small in the perturbation amplitude as it goes to zero.

We have determined that there are two modes of merger: inside the separatrix, points merge if they are within a critical merger distance; outside the separatrix, points merge if the shear stretches the vortices out and brings them together with an appropriate orientation. (This is made particularly clear by Figs. 5 and 6.) A merger criterion for the first mode

can be determined directly from the Poincaré section, but the second mode is not so easily characterized. Moreover, the relationship between the separatrix splitting and vortex merger is not a simple one. While numerical computations confirm that the separatrix splitting is small, it has been observed that widely separated vortices can merge. On the corresponding trajectories, the aspect ratios of the vortices are not $O(1)$ when the separatrix is crossed, but much less; the trajectories do not cross the separatrix so much as they burrow underneath it (in the 3-D phase space). In effect, the merging trajectories live on a different part of the Hamiltonian surface. Evidence for the importance of the separatrix splitting is at best negative: merger does not occur for trajectories where $\lambda = O(1)$.

The Hamiltonian moment formulation clarifies some aspects of MZS's formulation and it could also be used to derive higher order models (i.e. beyond the elliptical vortex approximation). Another advantage of the Hamiltonian approach is that it enables one to explain certain aspects of the dynamics by appealing to the topology of those surfaces. Also, it is preferable to define a merger criterion for noncircular vortices at fixed H_0 rather than fixed λ, especially when H_0 has a simple physical interpretation.

Our analysis has been restricted to the simplest possible case of two identical vortices. Furthermore, we have only considered a linear shear flow in our numerical computations. It would be interesting to see what happens when these restrictions are relaxed. Indeed, by considering a wider range of cases, it may be possible to find a situation wherein the separatrix splitting does have a direct effect on vortex merger.

APPENDIX: A PAIR OF POINT VORTICES IN SHEAR

The equations of motion for N point vortices in a steady background flow $\mathbf{u}(\boldsymbol{x}_i)$ are given by

$$\dot{\boldsymbol{x}}_i = \frac{\Gamma_i}{2\pi} \sum_{j=1}^{N}{}' \frac{\mathbf{k} \times (\boldsymbol{x}_i - \boldsymbol{x}_j)}{\mid \boldsymbol{x}_i - \boldsymbol{x}_j \mid^2} + \mathbf{u}(\boldsymbol{x}_i), \tag{A1}$$

where $\mathbf{k} \times (x_i, y_i) = (-y_i, x_i)$. For $N = 2$ vortices and a background flow given by (11), i.e.

$$(u, v) = \left(-\tfrac{1}{2}(\omega - e)y, \tfrac{1}{2}(\omega + e)x\right), \tag{A2}$$

the equations of motion may be written in the form

$$\dot{x}_1 = -\frac{\Gamma_2}{2\pi} \frac{y_1 - y_2}{\mid \boldsymbol{x}_1 - \boldsymbol{x}_2 \mid^2} - \tfrac{1}{2}(\omega - e)y_1 \tag{A3}$$

$$\dot{y}_1 = \frac{\Gamma_2}{2\pi} \frac{x_1 - x_2}{\mid \boldsymbol{x}_1 - \boldsymbol{x}_2 \mid^2} + \tfrac{1}{2}(\omega + e)x_1$$

$$\dot{x}_2 = -\frac{\Gamma_1}{2\pi} \frac{y_2 - y_1}{\mid \boldsymbol{x}_1 - \boldsymbol{x}_2 \mid^2} - \tfrac{1}{2}(\omega - e)y_2$$

$$\dot{y}_2 = \frac{\Gamma_1}{2\pi} \frac{x_2 - x_1}{\mid \boldsymbol{x}_1 - \boldsymbol{x}_2 \mid^2} + \tfrac{1}{2}(\omega + e)x_2.$$

Defining $X = x_1 - x_2$, $Y = y_1 - y_2$, and nondimensionalizing time by $(\Gamma_1 + \Gamma_2)^{-1}$, the equations for the vortex separation are

$$\dot{X} = -\left(\frac{1}{2\pi} \frac{1}{X^2 + Y^2} + \tfrac{1}{2}(\omega - e)\right) Y \tag{A4}$$

$$\dot{Y} = \left(\frac{1}{2\pi} \frac{1}{X^2 + Y^2} + \tfrac{1}{2}(\omega + e)\right) X.$$

where now $\omega := \omega/(\Gamma_1 + \Gamma_2), e := e/(\Gamma_1 + \Gamma_2)$.

There are two types of fixed points for the preceding equations:

$$I: \qquad X = 0, \;\; Y = \pm\left(-\frac{1}{\pi} \frac{1}{\omega - e}\right)^{\frac{1}{2}} \tag{A5}$$

$$II: \qquad X = \pm\left(-\frac{1}{\pi} \frac{1}{\omega + e}\right)^{\frac{1}{2}}, \;\; Y = 0.$$

Type I is present if $\omega - e < 0$, and type II is present if $\omega + e < 0$. Linearizing around the fixed points, it is easily shown that type I are hyperbolic, and type II are elliptic.

The hyperbolic fixed points are connected by a separatrix (see Fig. 1). The separatrix is defined implicitly by the Hamiltonian

$$H = \frac{\Gamma_1\Gamma_2}{2\pi} \ln \mid \boldsymbol{x}_1 - \boldsymbol{x}_2 \mid + \frac{1}{4}(\omega - e)(\Gamma_1 y_1^2 + \Gamma_2 y_2^2) + \frac{1}{4}(\omega + e)(\Gamma_1 x_1^2 + \Gamma_2 x_2^2). \qquad \text{(A6)}$$

For $\Gamma_1 = \Gamma_2 = 1$ and $(e, \omega) = (1/\pi, -1/\pi)$, the hyperbolic fixed points are located at $(0, \pm 1)$.

REFERENCES

1. S. Kida, "Motion of an elliptic vortex in a uniform shear flow," J. Phys. Soc. Jpn. **50**, 3517 (1981).

2. M.V. Melander, N.J. Zabusky, and A.S. Styzeck, "A moment model for vortex interactions of the two-dimensional Euler equations. Part 1: computational validation of a Hamiltonian elliptical representation," J. Fluid Mech. **167**, 95 (1986).

3. G.R. Flierl, S.P. Meacham, and P.J. Morrison, preprint (1995).

4. B.J. Hoskins, M.E. McIntyre, and A.W. Robertson, "On the use and significance of isentropic potential vorticity maps," Q.J. Roy. Met. Soc. **111**, 877 (1985).

5. W.R. Holland, T. Keffer, and P.B. Rhines, "Dynamics of the oceanic general circulation: the potential vorticity field," Nature **308**, 698 (1984).

6. K. Shultz-Tokos and T. Rossby, "Kinematics and dynamics of a Mediterranean salt lens," J. Phys. Oceanogr. **21**, 879 (1991).

7. C. Basdevant, B. Legras, R. Sadourny, and M. Béland, "A study of barotropic model flows, intermittency, waves and predictability," J. Atmos. Sci. **36**, 2305 (1981).

8. J.C. McWilliams, "The emergence of isolated vortices in turbulent flow," J. Fluid Mech. **146**, 21 (1984).

9. J.C. McWilliams, "The vortices of two-dimensional turbulence," J. Fluid Mech. **219**, 361 (1990).

10. K.V. Roberts and J.P. Christiansen, "Topics in computational fluid mechanics," Comp. Phys. Commun. **3** (Suppl.), 14 (1972).

11. M.V. Melander, N.J. Zabusky, and J.C. McWilliams, "Symmetric vortex merger in two dimensions: causes and conditions," J. Fluid Mech. **195**, 303 (1988).

12. D.G. Dritschel and B. Legras, "The elliptical model of two-dimensional vortex dynamics. II. Disturbance equations," Phys. Fluids A **3**, 855 (1991).

13. P.J. Morrison and J. M. Greene, "Noncanonical Hamiltonian density formulation of hydrodynamics and ideal magnetohydrodynamics," Phys. Rev. Lett. **45**, 790 (1980).

14. P.J. Morrison, "Hamiltonian description of the ideal fluid" in *Geophysical Fluid Dynamics; Proc. 1993 WHOI Summer Program,* eds. R. Salmon and B. Ewing-Deremer (Woods Hole Oceanogr. Inst. Technical Report WHOI-94-12, Woods Hole, MA, 1994).

15. R. Salmon, "Hamiltonian fluid mechanics," Ann. Rev. Fluid Mech. **20**, 225 (1988).

16. T.G. Shepherd, "Symmetries, conservation laws and Hamiltonian structure in geophysical fluid dynamics," Adv. Geophys. **32**, 287 (1990).

17. P.J. Morrison, "Poisson brackets for fluids and plasmas" in *Mathematical Methods in Hydrodynamics and Integrability in Related Dynamical Systems,* AIP Conf. Proc. **88**, 13 (1982).

18. R.D. Hazeltine, C.T. Hsu, and P.J. Morrison, "Hamiltonian four-field model for nonlinear tokamak dynamics," Phys. Fluids **30**, 3204 (1987).

19. J.E. Marsden and A. Weinstein, "Reduction of Manifolds with Symmetry," Rep. Math. Phys. **5**, 121 (1974).

20. V.I. Arnold, V.V. Kozlov, and A.I. Neishtadt, *Mathematical Aspects of Classical and Celestial Mechanics: Encyclopedia of Mathematical Sciences III* (Springer-Verlag, Berlin, 1988).

21. After a preliminary version of this work had been published [K. Ngan, "Elliptical vortices in shear: Hamiltonian formulation, vortex merger, and chaos"; see Ref. 14, pp. 211–221] we learned that Hamiltonian reduction had been independently used in the context of the MZS model by A. Rouhi (see Ref. 27, pp. 278-285).

22. S. Wiggins, *Introduction to Applied Nonlinear Dynamical Systems* (Springer-Verlag, New York, 1990).

23. R.S. MacKay, J.D. Meiss, and I.C. Percival, "Transport in Hamiltonian systems," Physica D **13**, 55 (1984).

24. D. Bensimon and L.P. Kadanoff, "Extended chaos and disappearance of KAM trajectories," Physica D **13**, 82 (1984).

25. S. Wiggins, *Chaotic Transport in Dynamical Systems* (Springer-Verlag, New York, 1992).

26. P. Holmes, J. Marsden, and J. Scheurle, "Exponentially small splittings of separatrices with applications to KAM theory and degenerate bifurcations," Contemp. Math. **81**, 213 (1988).

27. P.G. Saffman, *Vortex Dynamics* (Cambridge University Press, Cambridge, 1992).

28. H. Aref and N. Pomphrey, "Integrable and chaotic motion of four vortices. I. The case of identical vortices," Proc. Roy. Soc. Lond. A **380**, 359 (1982).

29. R.S. MacKay and J.D. Meiss (eds.), *Hamiltonian Dynamical System: A Reprint Selection* (Adam Hilger, Bristol, 1987).

30. J. Guckenheimer and P. Holmes, *Nonlinear Oscillations, Dynamical Systems, and Bifurcations of Vector Fields* (Springer-Verlag, New York, 1983).

31. P.G. Drazin, *Nonlinear Systems* (Cambridge University Press, Cambridge, 1992).

32. J. Scheurle, J.E. Marsden and P. Holmes, "Exponentially small estimates for separatrix splittings," in *Asymptotics Beyond All Orders,* eds. H. Segur *et al.* (Plenum, New York, 1991).

33. M. Kummer, J.A. Ellison, and A.W. Sáenz "Exponentially small phenomena in the rapidly forced pendulum," in *Asymptotics Beyond All Orders,* eds. H. Segur *et al.* (Plenum, New York, 1991).

34. A. Erdélyi, *Asymptotic Expansions* (Dover, New York, 1956).

35. For non-merging trajectories, ϕ increases monotonically with time, as was assumed in the Melnikov analysis.

36. D.W. Waugh, "Forced vortex merger," in *Geophysical Fluid Dynamics; Proc. 1991 WHOI Summer Program,* eds. W. Young and S. Meacham (Woods Hole Oceanogr. Inst. Technical Report WHOI-92-16, Woods Hole, MA, 1992).

37. A.J. Lichtenberg and M.A. Lieberman, *Regular and Chaotic Dynamics,* 2nd ed. (Springer-Verlag, New York, 1992).

38. U. Smilansky "The classical and quantum theory of chaotic scattering" in *Chaos and Quantum Physics*, Proc. Les Houches Session LII, eds. M.-J. Giannoni *et al.* (Elsevier, Amsterdam, 1992).

39. E. Ott and T. Tél, "Chaotic scattering: an introduction," Chaos **3**, 417 (1993).

40. B. Eckhardt and H. Aref, "Integrable and chaotic motions of four vortices. II. Collision dynamics of vortex pairs," Phil. Trans. R. Soc. Lond. A **326,** 655 (1988).

41. T. Price, "Chaotic scattering of two identical point vortex pairs," Phys. Fluids A **5**, 2479 (1993).

42. K. Ide and S. Wiggins, "The dynamics of elliptically shaped regions of uniform vorticity in time-periodic, linear external velocity fields," *Fluid Dynamics Research* **15**, 205 (1995).

FIGURE CAPTIONS

FIG. 1. Phase space geometry for a point vortex pair in shear.

FIG. 2. Hamiltonian surfaces for $\Gamma = 1$ and $(x_0, y_0, \lambda_0) = (0, 1, 1.5)$. a) MZS model, i.e. $A = \pi/100$ or $\epsilon = 0.01$. b) $\epsilon = 0.01$ and $(\omega, e) = (-1/\pi, 1/\pi)$.

FIG. 3. Poincaré sections corresponding to the Hamiltonian surfaces of Fig. 2. a) MZS model ($\epsilon = 0.01$, no shear). b) $\epsilon = 0.01$ with shear. c) $\epsilon = 0.03$ with shear.

FIG. 4. Typical merging trajectory for $\epsilon = 0.01$ and $(\omega, e) = (-1/\pi, 1/\pi)$. The initial conditions are $(r_i, \theta_i, \lambda_i) = (0.400, 1.57, 0.111)$. This is an example of the vortex-vortex mode of merger. (For convenience, t is scaled by $q_0 = 100/\pi$.)

FIG. 5. Merging initial conditions well-outside the separatrix plotted on top of a 2-D projection of the Hamiltonian surface. $\epsilon = 0.01$ and $(\omega, e) = (-1/\pi, 1/\pi)$.

FIG. 6. Typical merging trajectory corresponding to Fig. 5. a) $r : t$; and b) $\lambda : t$. The initial conditions are $(r_i, \theta_i, \lambda_i) = (9.00,\ 2.81,\ 0.0102)$. This is an example of shear-induced merger. (For convenience, t is scaled by $q_0 = 100/\pi$.)

FIG. 7. Blow-up of region around the separatrix for $\epsilon = 0.01$. a) Poincaré section for initial conditions $(r_i, \theta_i) = (0.99 - 1.01,\ \pi/2)$. b) Typical trajectory just inside the separatrix: $(r_i, \theta_i, \lambda_i) = (0.998, 1.57, 0.7255)$. Other parameters as in Fig. 2. (For convenience, t is scaled by $q_0 = 100/\pi$.)

FIG. 8. Chaos in the interior for $\epsilon = 0.01$. a) Poincaré section for $r = 0.40 - 0.50$. b) Typical "chaotic" trajectory. The initial conditions are $(r_i, \theta_i, \lambda_i = (0.45, 0.00,\ 0.152)$. Other parameters as in Fig. 2. (For convenience, t is scaled by $q_0 = 100/\pi$.)

FIG. 9. Chaotic scattering around the separatrix for $\epsilon = 0.01, r_i = 1.1$. a) Scattering angle θ_s vs. incident angle θ_i. b) Residence time vs. θ_i. c) Expanded view of θ_s vs. θ_i for $\theta_i \in (\pi/2, 1.68)$. Other parameters as in Fig. 2. (For convenience, t is scaled by $q_0 = 100/\pi$.)

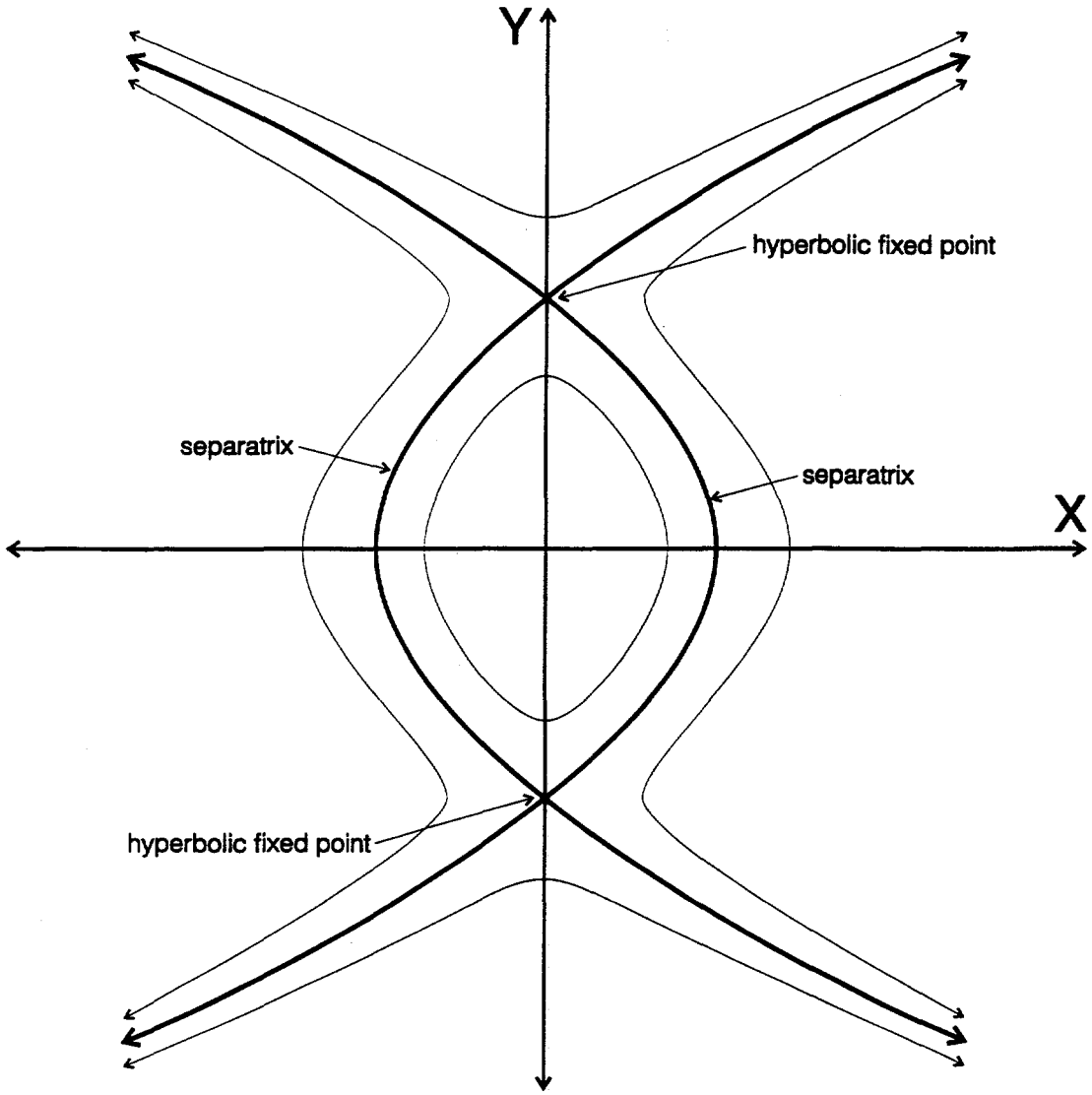
Y
X
hyperbolic fixed point
separatrix
separatrix
hyperbolic fixed point

Fig. 1

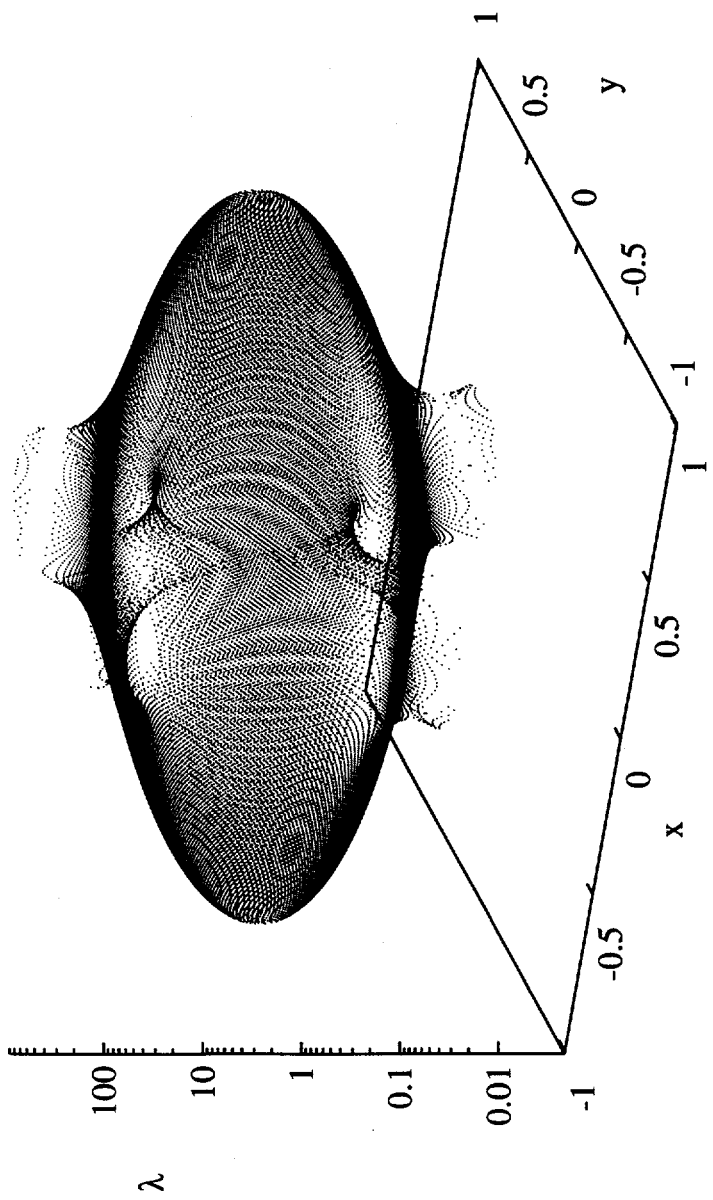

Fig. 2a

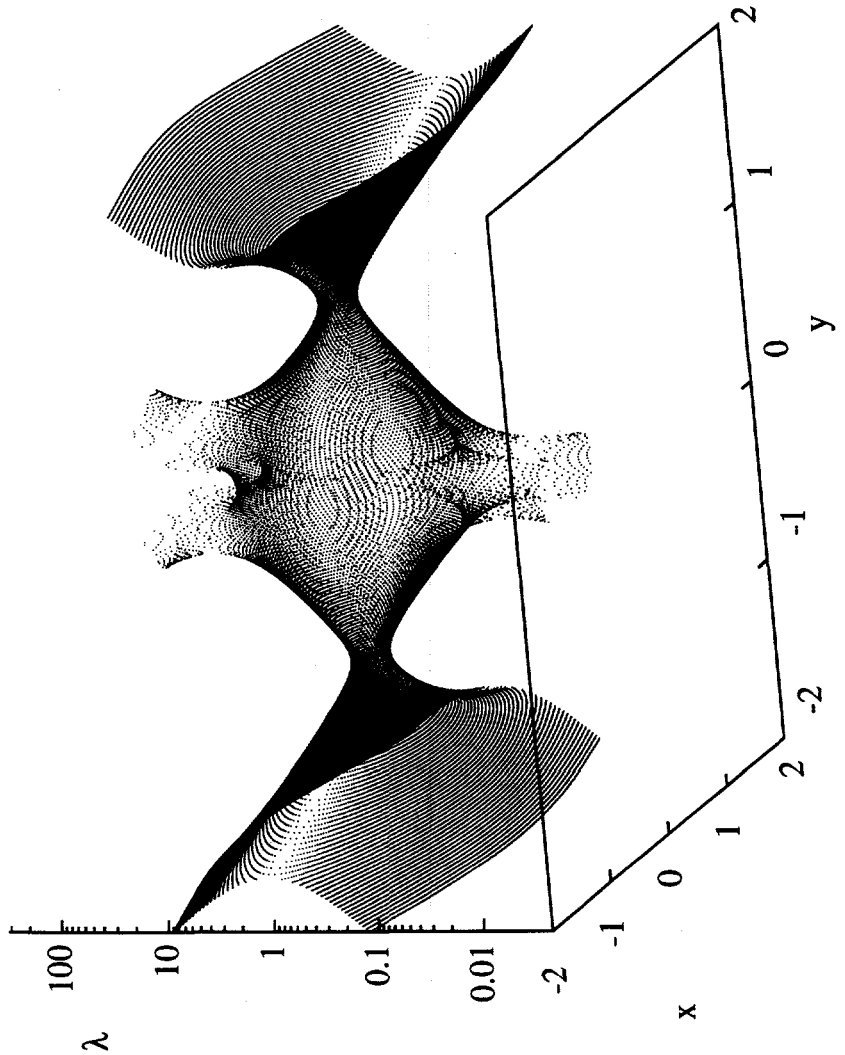

Fig. 2b

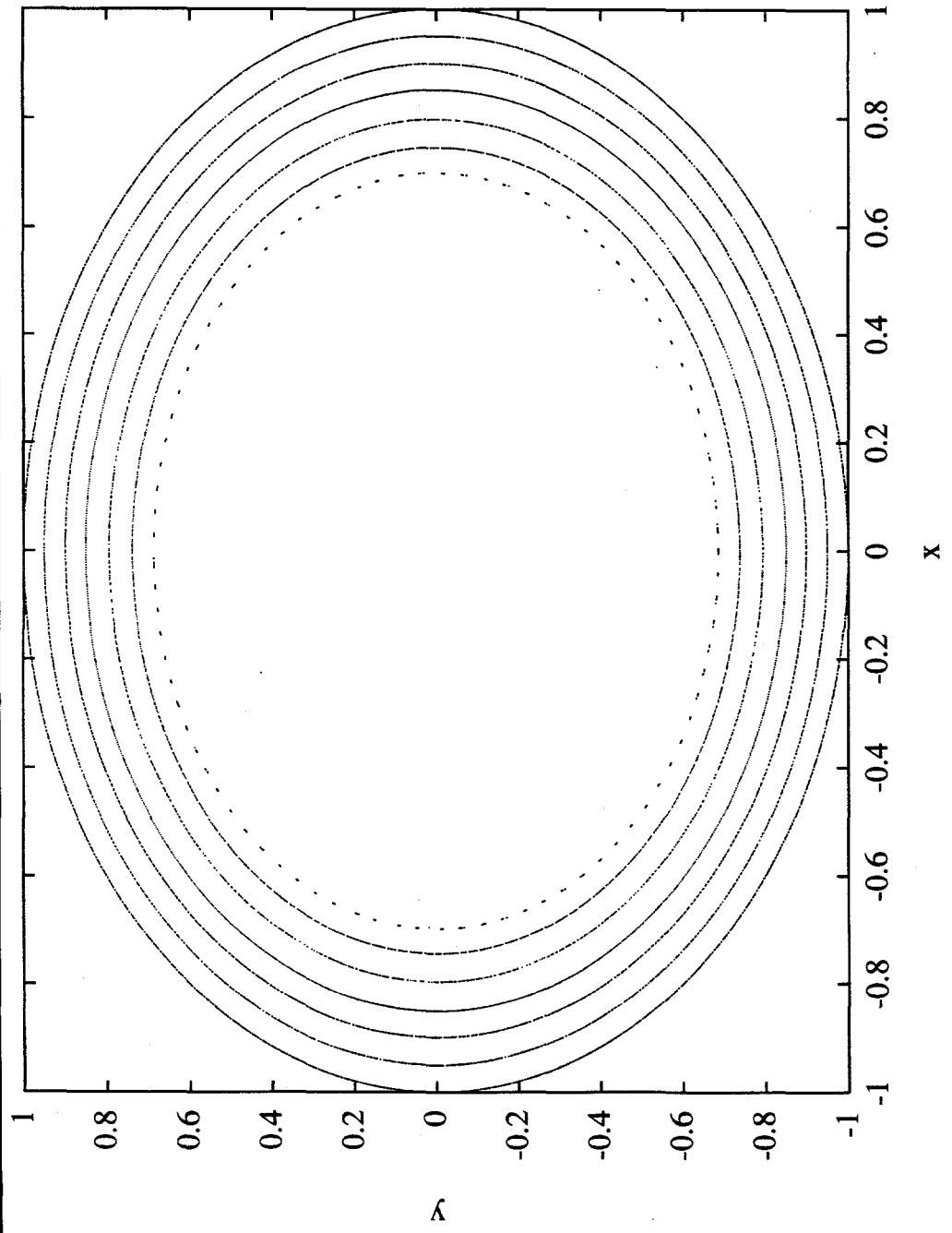

Fig. 3a

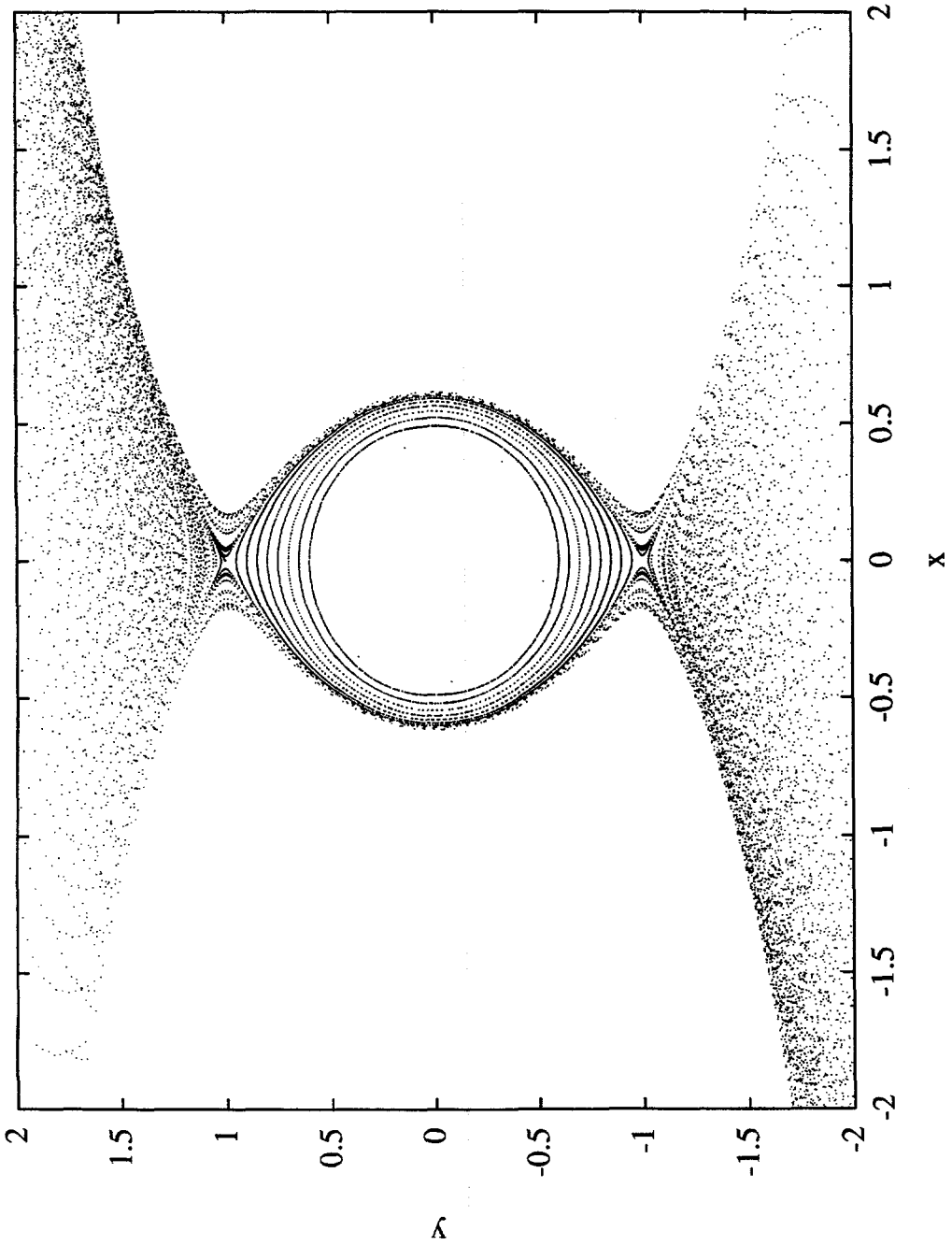

Fig. 3b

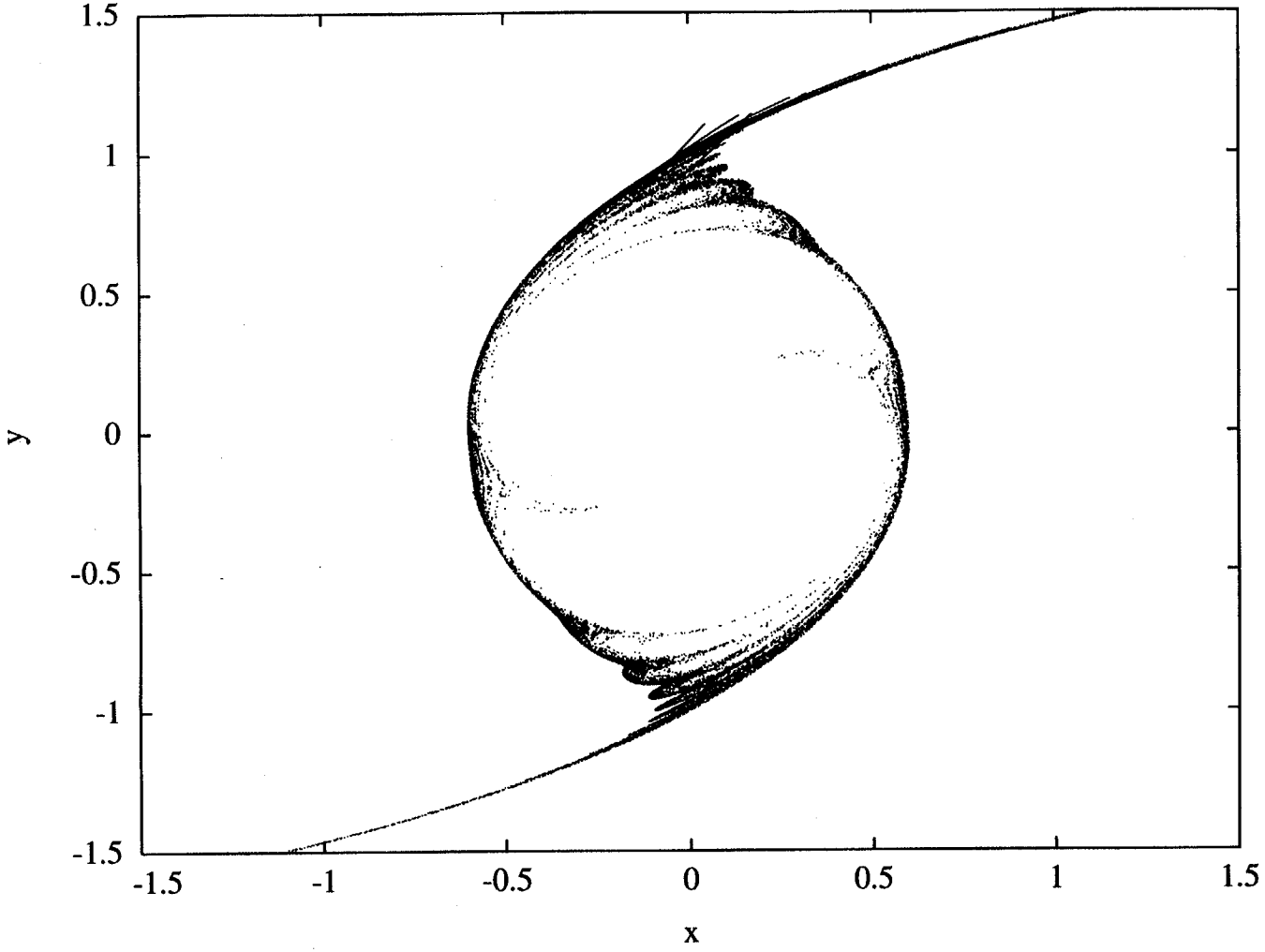

Fig. 3c

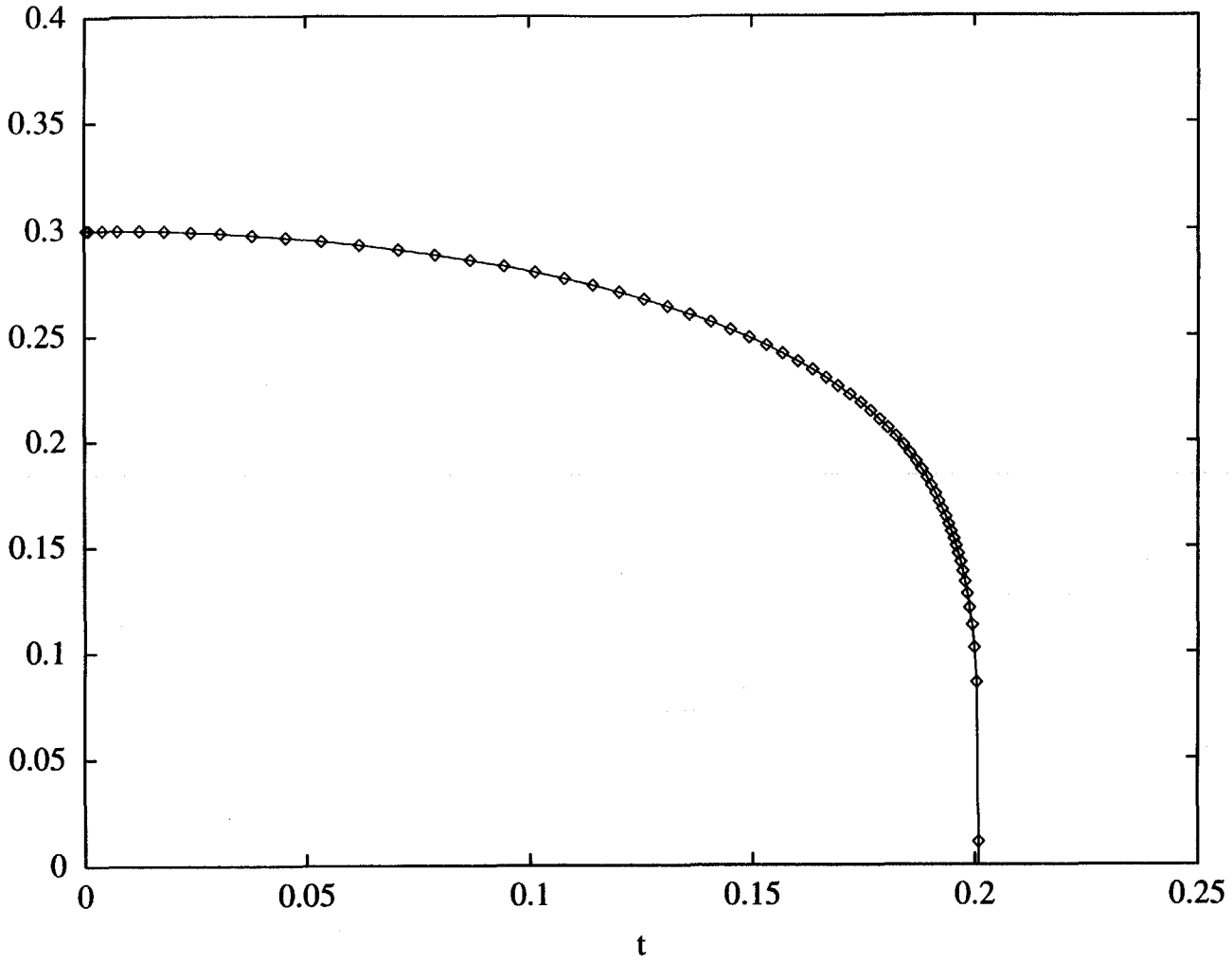

Fig. 4

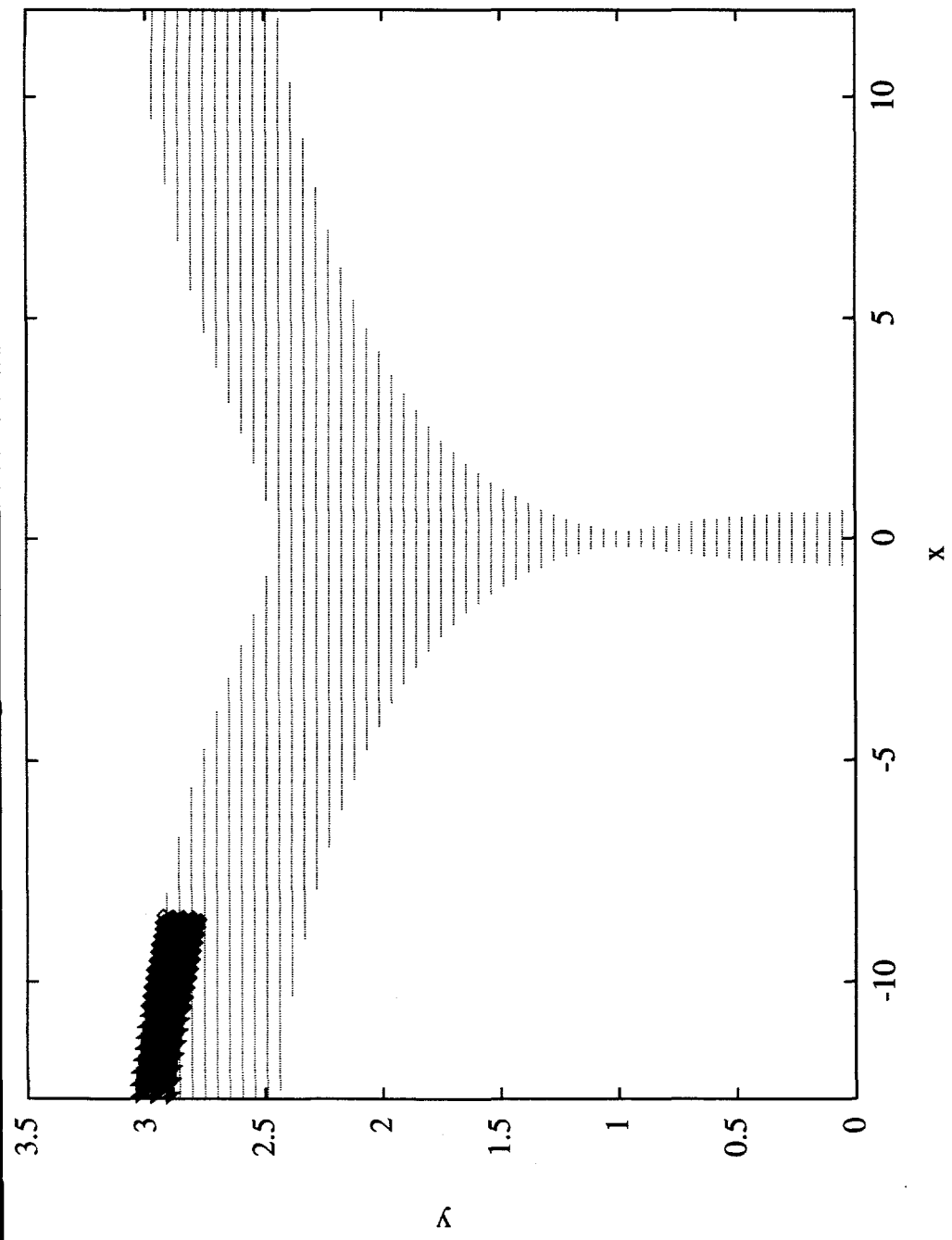

Fig. 5

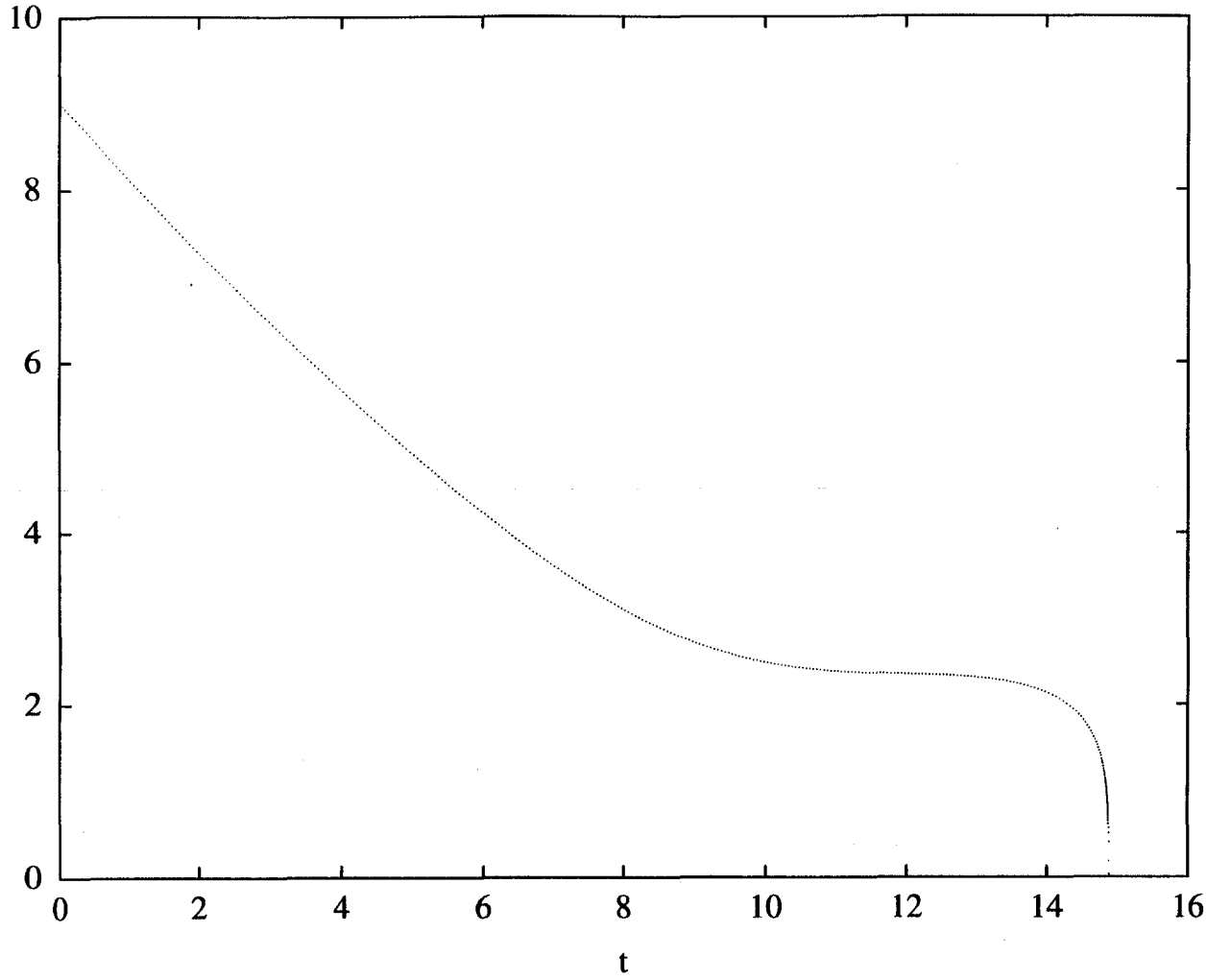

Fig. 6a

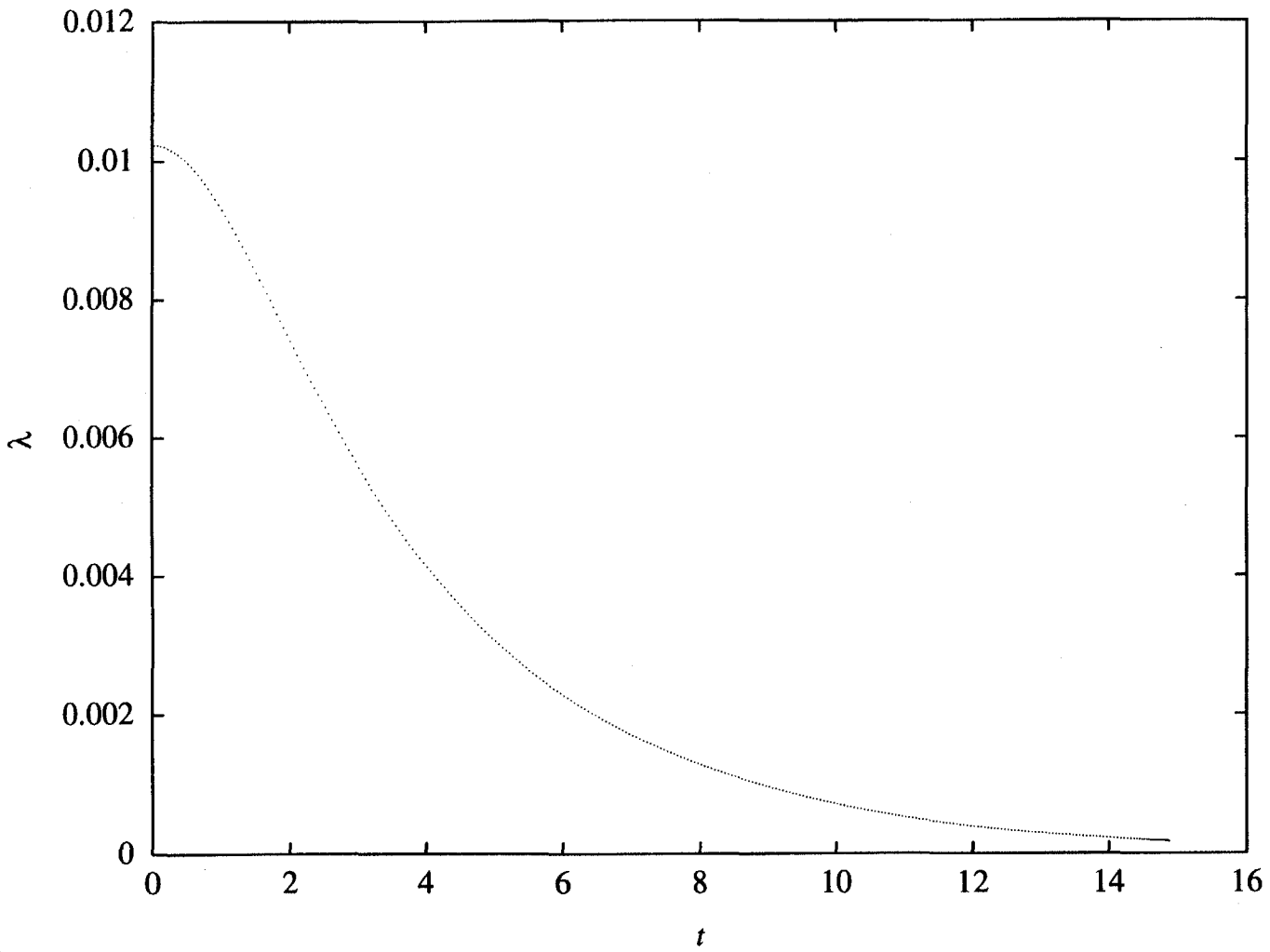

Fig. 6b

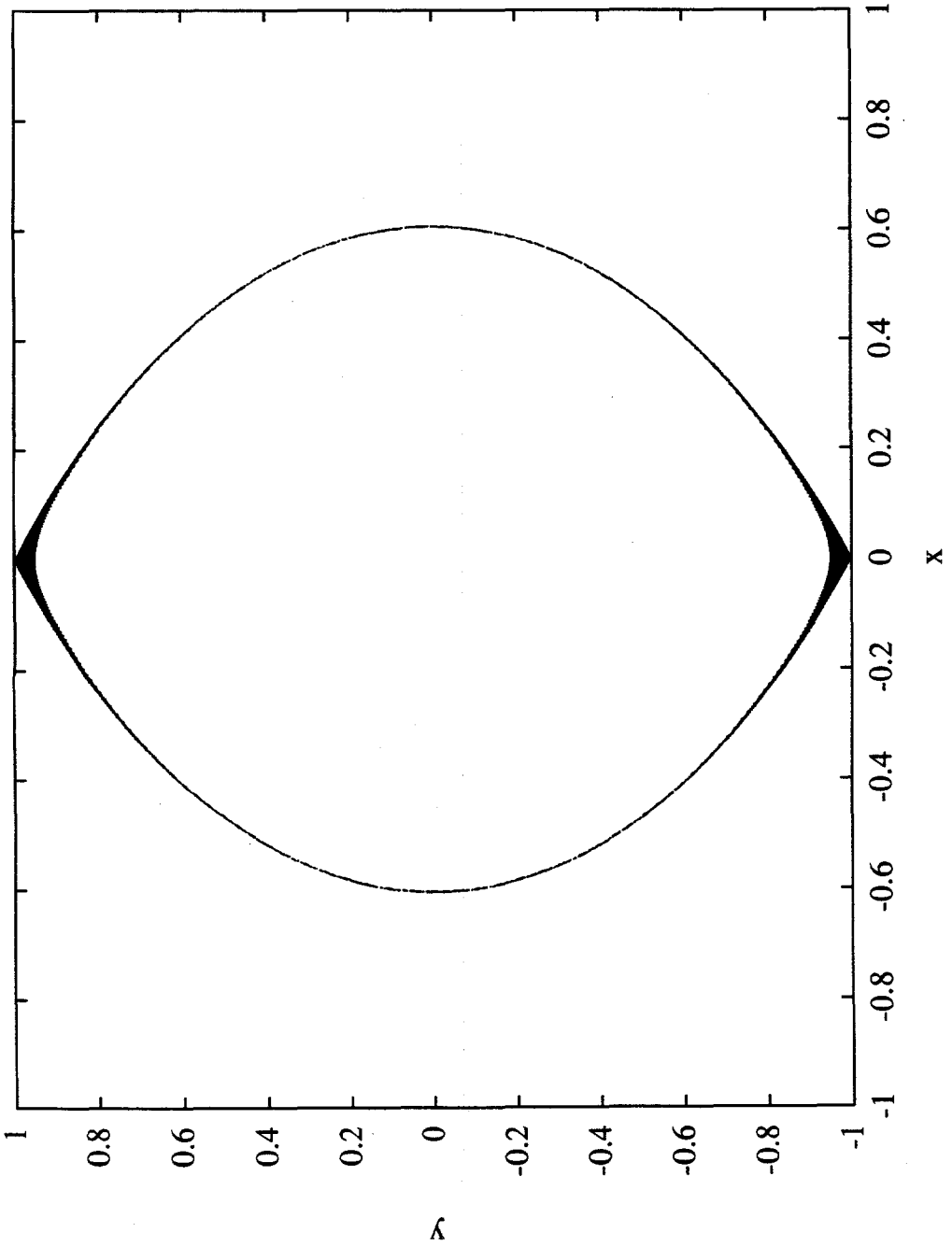

Fig. 7a

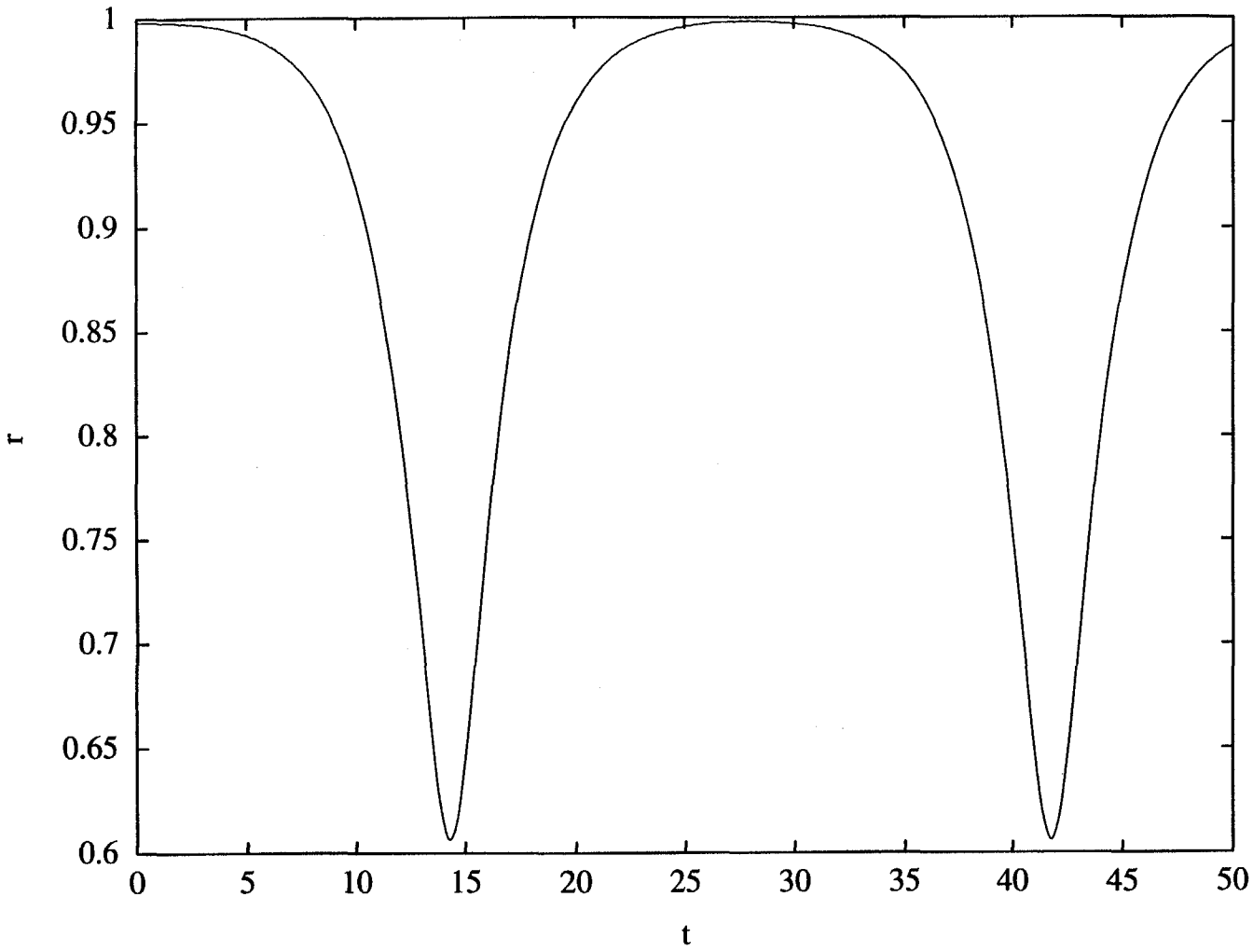

Fig. 7b

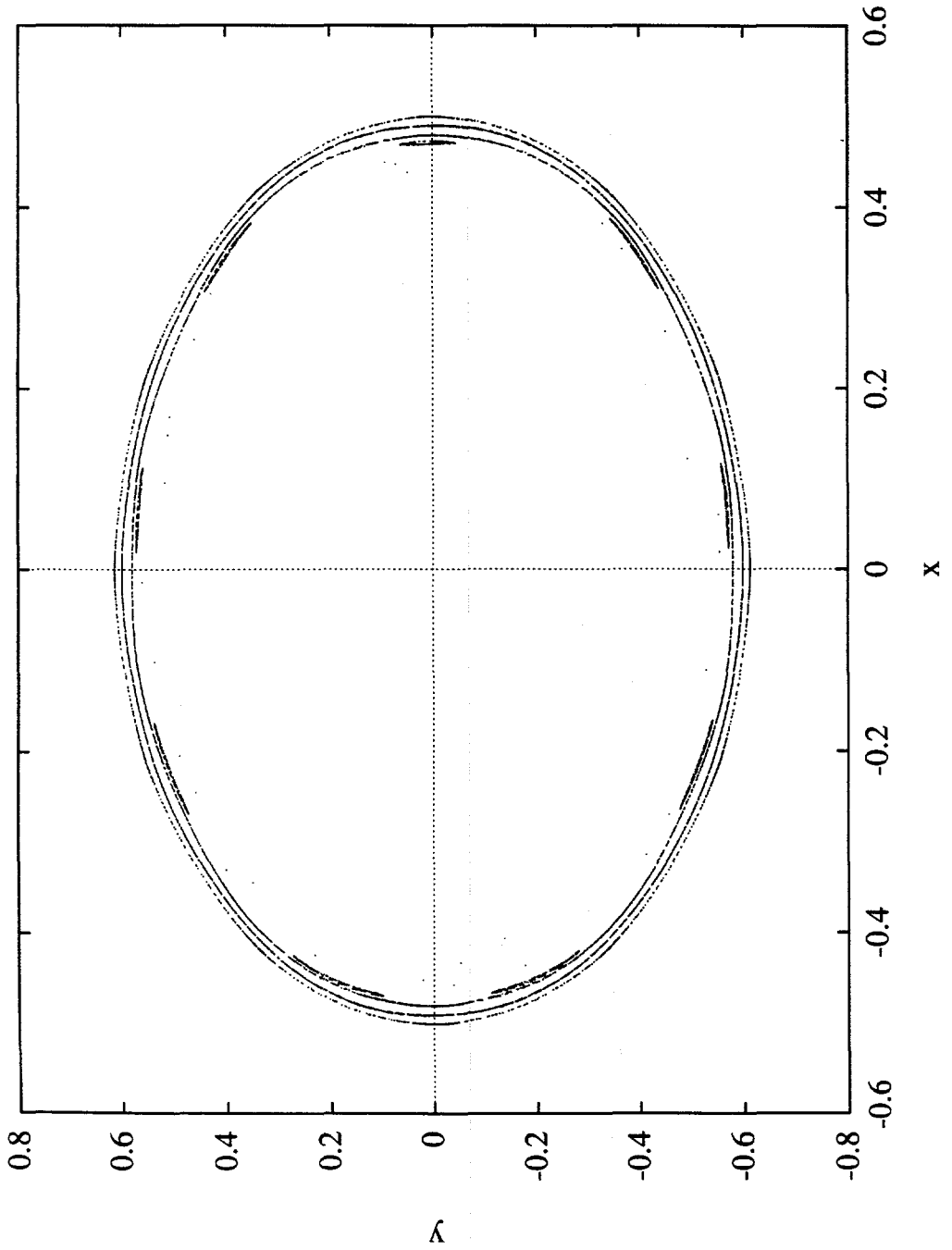

Fig. 8a

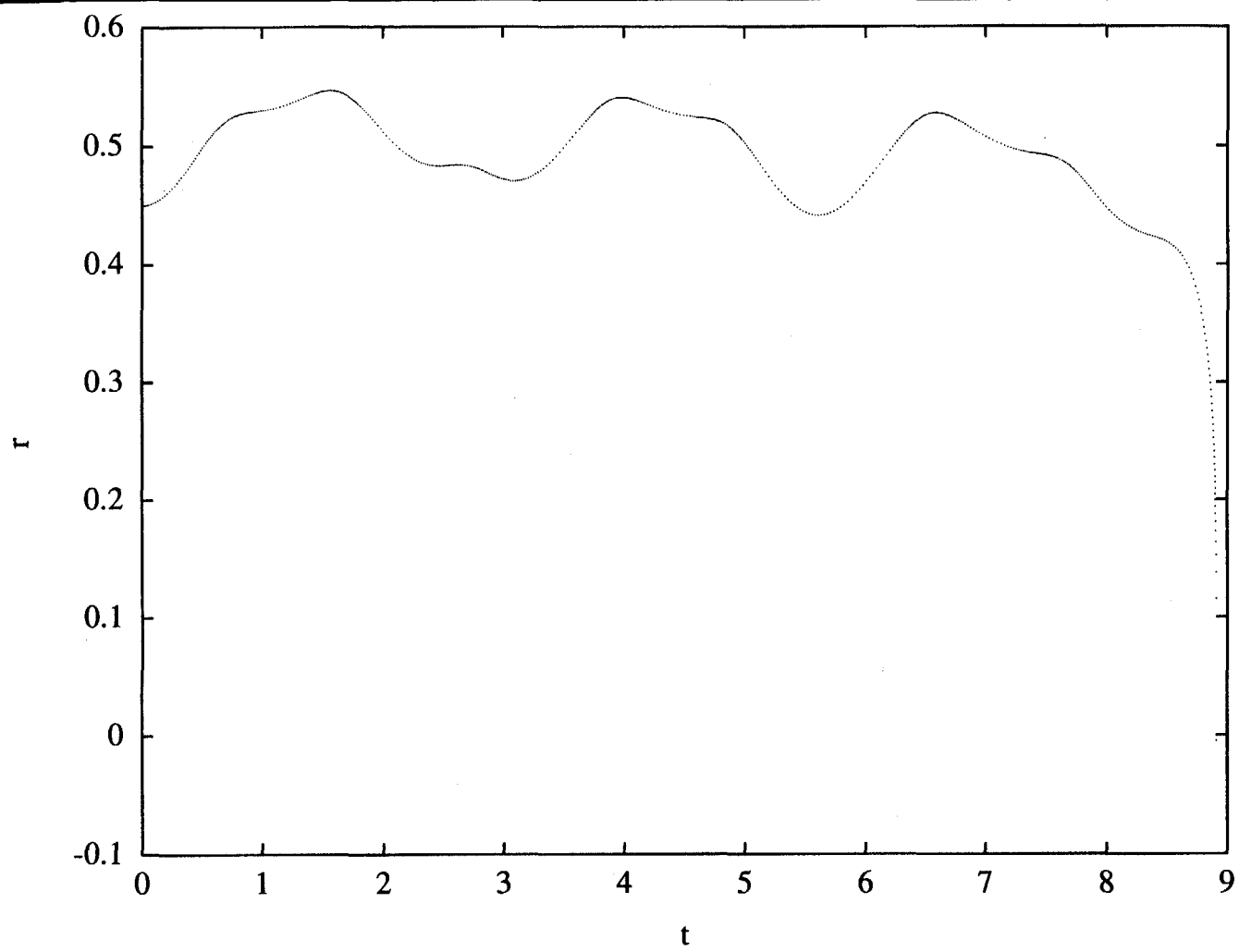

Fig. 8b

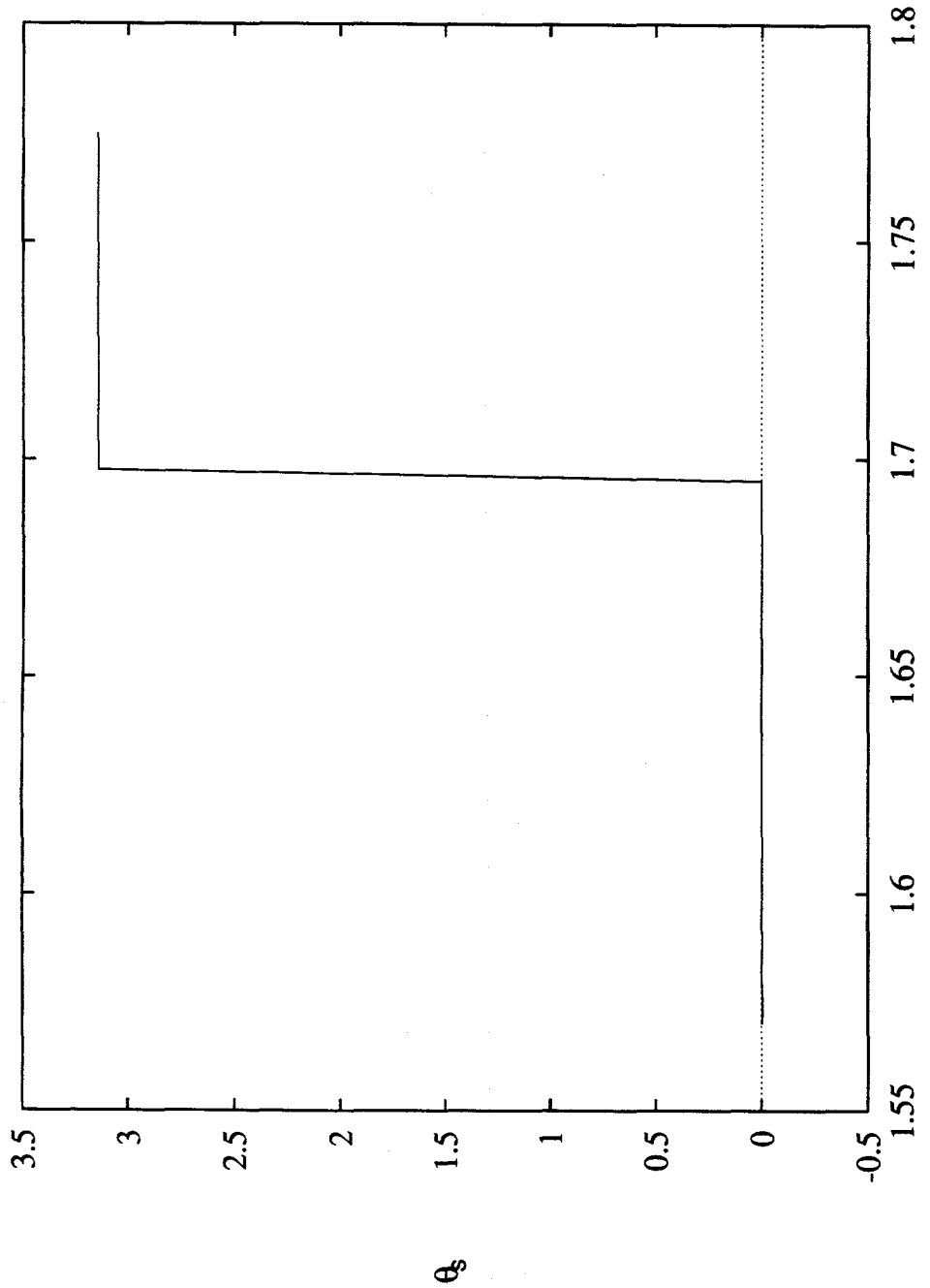

Fig. 9a

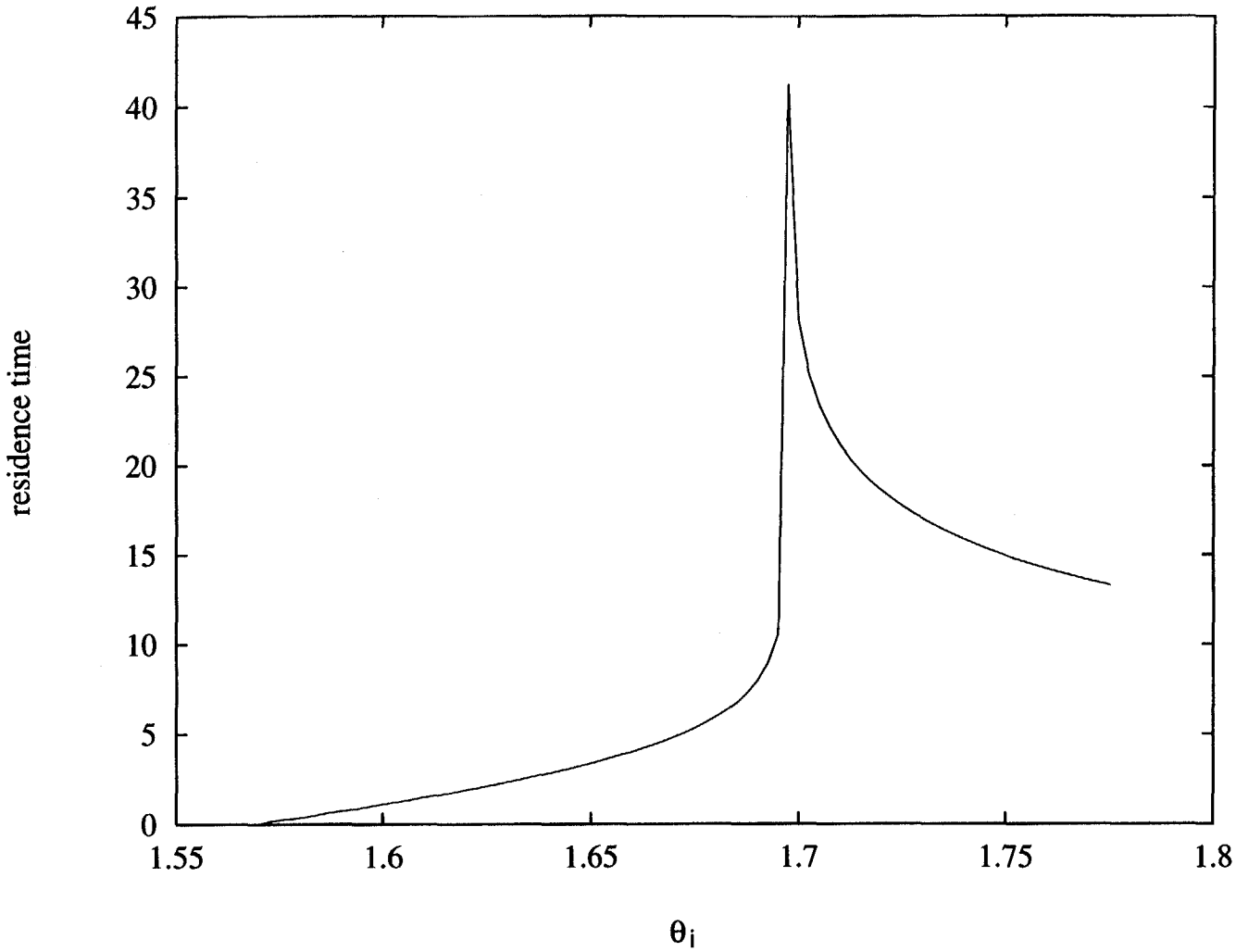
45
40
35
30
25
20
15
10
5
0
residence time
1.55
1.6
1.65
1.7
1.75
1.8
θ_i

Fig. 9b

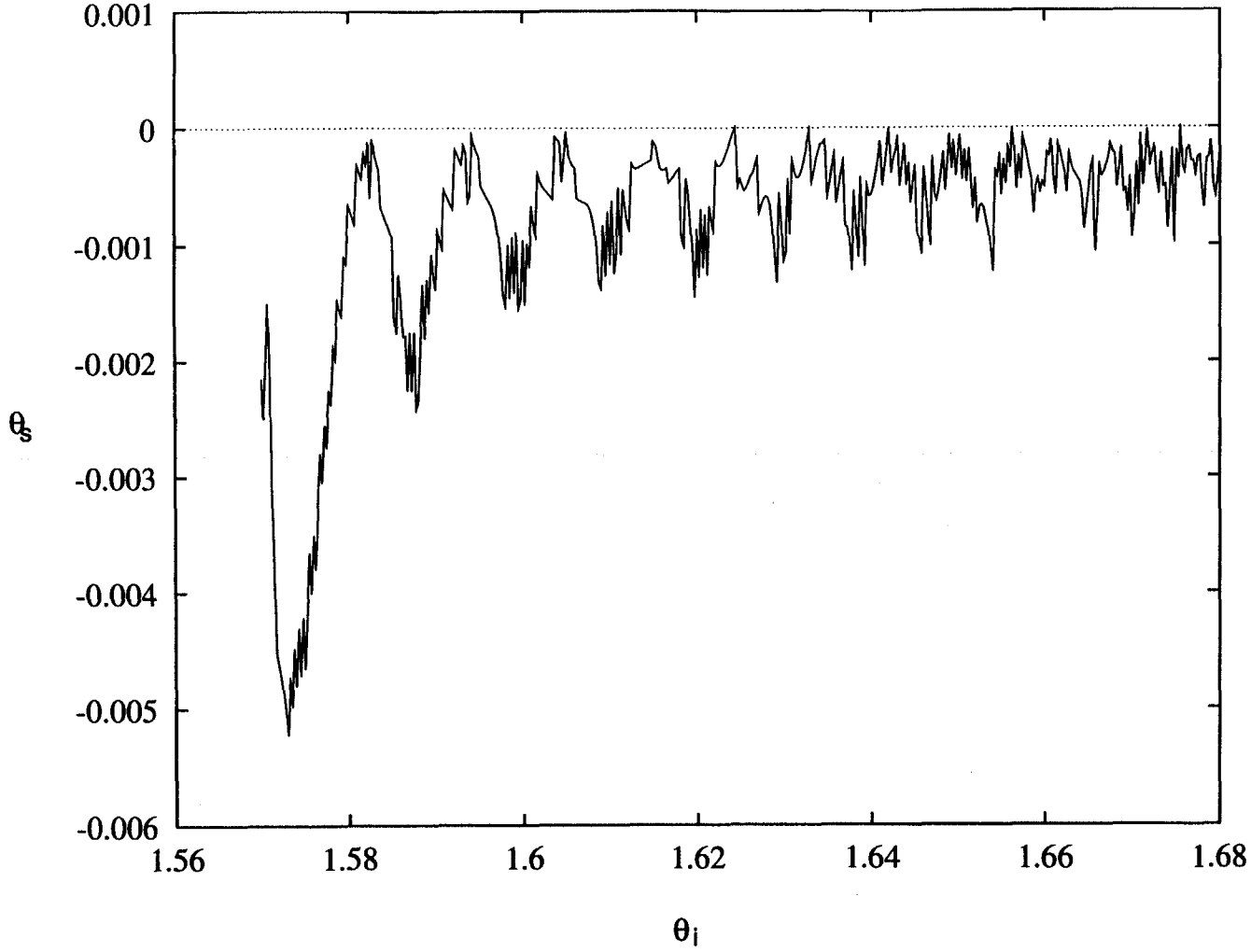
0.001
0
-0.001
-0.002
-0.003
-0.004
-0.005
-0.006
θ_s
1.56
1.58
1.6
1.62
1.64
1.66
1.68
θ_i

Fig. 9c